



Nomadic Use of a Plant Model - NOSE

Evaluation of Positioning Techniques in Industrial Environment

Authors: Heli Kokkoniemi-Tarkkanen, Paul Kemppi

Confidentiality: Public

Report's title Evaluation of Positioning Techniques in Industrial Environment		
Customer, contact person, address Tekes and Companies		Order reference
Project name Nomadic Use of a Plant Model		Project number/Short name NOSE
Author(s) Heli Kokkoniemi-Tarkkanen, Paul Kemppi		Pages 67/
Keywords Indoor positioning, WLAN fingerprinting, pseudolites, PDR, INS mechanization, sensor, AR/VR		Report identification code VTT-R-02103-09
Summary NOSE project studied methods and tools for ubiquitous plant model usage. Location aware services, augmented and virtual reality (AR/VR) techniques were studied in process industry surroundings in order to provide plant model services to a mobile device. This document describes the pilot carried out in Kvarnsveden, a paper mill in Sweden. It also describes positioning theory and preliminary trials behind it. Existing positioning solutions based on different technologies were shortly reviewed and their usability and limitations for the use cases were analysed. Three of the solutions were chosen for the first trial in 2008. WLAN location fingerprinting, pseudolites, and inertial navigation methods were implemented and tested in an authentic environment. Results show that WLAN positioning provides coarse positioning accuracy and thus, it can be used as a complementary positioning system. Moreover, the first trial and pre-trials indicated that setting up a pseudolite positioning system requires a lot of planning and adjustments. However, when the installation is final, the system stays well synchronized unless the direct signal between the reference antenna and the pseudolites is blocked. If the space is large and high enough and the pseudolite constellation is good, the pseudolite system offers pretty good tracking in open areas. Unfortunately, the equipment still sets limits on effective usage. Inertial navigation yielded good tracking accuracy, but requires periodic location fixes.		
 Based on the experiences from the first trials, a hybrid positioning solution was implemented and tested in the second trial in 2009. Hybrid solution combines Pedestrian Dead Reckoning (PDR) and coarse WLAN positioning with marker-less vision based tracking. The idea of marker-less vision based tracking is to compare current camera view with images collected earlier from the environment. During the image database collection phase, location information and WLAN signal level data is assigned for each of the images. During positioning phase, WLAN positioning is used to limit the image database search and lower the risk of finding ambiguous image matches. Location fixes from marker-less tracking are then used to aid PDR to get smooth and continuous estimate of the user location. Results from the last trial show that the implemented solution outperforms the methods evaluated in the first trial and thus is a promising candidate for indoor positioning in complex industrial environments.		
Confidentiality	Public	
Espoo 11.1.2010		
Signatures	Signatures	Signatures
Written by Senior Research Scientist Heli Kokkoniemi-Tarkkanen	Reviewed by Research Professor Tommi Karhela	Accepted by Technology Manager Jari Hämäläinen
VTT's contact address PL 1000, Vuorimiehentie 3, 02044 – VTT		
Distribution Tekes, Pöyry Forest Industry, Fortum Nuclear Services, Nokia Research Center, Metso Paper, Wärtsilä, Prowledge, Intergraph Finland, Cadmatic, Space Systems Finland, R.A. TRConsulting, VTT.		
<i>The use of the name of the VTT Technical Research Centre of Finland (VTT) in advertising or publication in part of this report is only permissible with written authorisation from the VTT Technical Research Centre of Finland.</i>		

Preface

This report summarises the results of positioning research and trials in *Nomadic Use of a Plant Model* (NOSE) project during January 2008 – December 2009. The project was funded by Tekes, Pöyry Forest Industry, Fortum Nuclear Services, Nokia Research Center, Metso Paper, Wärtsilä, Prowledge, Intergraph Finland, Cadmatic, Space Systems Finland, and R.A. TRConsulting. The objective of the positioning research was to explore existing positioning solutions based on different technologies and evaluate their usability for indoor positioning in industrial facility environment. The objective was also to test potential methods in paper mill trial and analyse both the limitations of the selected positioning solutions and the accuracy requirements for different use cases. Based on the experiences from the first trials, a hybrid positioning solution was implemented and tested in the second trial in 2009.

The project was led by Tommi Karhela. The research work and preparation of this report was done by Heli Kokkoniemi-Tarkkanen, Paul Kemppi, Juuso Pajunen and Yanli Li.

The project team acknowledges especially the members of ILPO and HYPEL for the valuable comments and efficient collaboration. In addition, the project team thanks Heikki Laitinen from Space Systems Finland and visiting researcher Christos Laoudias from University of Cyprus for their contribution to the pseudolite and WLAN positioning related research.

Espoo 11.1.2010

Authors

Abbreviation List

AP	Access Point
C/A	Clear/Acquisition
CAT	Category
CI	Cell Identity
DCM	Database Correlation Method
DOP	Dilution of Precision
DR	Dead Reckoning
EKF	Extended Kalman Filter
Galileo	European Global Navigation Satellite System
GNSS	Global Navigation Satellite System
GPS	Global Positioning System
GSM	Global System for Mobile communications
IMU	Inertial Measurement Unit
INS	Inertial Navigation System
IR	Infrared
LOS	Line of Sight
MCS	Master Control Station
MEMS	Microelectronic Mechanical System
MU	Mobile Unit
PCA	Principal Component Analysis
PDR	Pedestrian Dead Reckoning
PRN	Pseudo-Random Noise
RF	Radio Frequency
RFID	Radio-Frequency Identification
RP	Reference Point
RSS	Radio Signal Strength
RTCM	Radio Technical Commission for Maritime Services
RTLS	Real-Time Locating System
SMC	Sequential Monte Carlo
SNR	Signal to Noise Ratio
SSF	Space Systems Finland
UMTS	Universal Mobile Telecommunication System
USB	Universal Serial Bus
UWB	Ultra Wide Band
Wi-Fi	Wireless Fidelity
WLAN	Wireless LAN
ZUPT	Zero velocity Update

Contents

Preface	3
Abbreviation List	4
Contents	5
1 Introduction	7
2 Evaluated positioning methods and theory	9
2.1 WLAN signal strength based positioning indoors	9
2.1.1 Database Correlation Method	9
2.2 Pseudolite positioning	9
2.2.1 Pseudolite positioning systems	10
2.2.2 Synchronization	11
2.2.3 Known weaknesses	12
2.3 Inertial/magnetic sensor positioning	13
2.3.1 INS mechanization	13
2.3.2 ZUPT based Pedestrian Dead Reckoning (PDR)	13
2.3.3 Alternative solutions for PDR	14
2.4 Methods for data fusion and filtering	14
2.5 Hybrid positioning utilizing marker-less vision based tracking	15
3 Pre-trials	17
3.1 Digitalo pre-trial	17
3.1.1 Trial area	17
3.1.2 Trial setup	18
3.1.3 Pseudolite measurement results	21
3.1.4 WLAN location fingerprinting results	27
3.1.5 Sensor navigation results	29
3.1.6 Combining WLAN location fingerprinting and sensor navigation	31
3.2 Preliminary trial in an underground facility	33
3.2.1 Trial area	33
3.2.2 Trial setup	34
3.2.3 Pseudolite measurement results	36
3.2.4 WLAN location fingerprinting results	44
4 Kvarnsveden pilot 2008	46
4.1 Trial area	46
4.2 Trial setup	47
4.3 Pseudolite measurement results	51
4.4 WLAN location fingerprinting results	56
4.5 Sensor navigation results	58
5 Kvarnsveden pilot 2009	60

5.1 Trial area	60
5.2 Trial setup	60
5.3 Reference image database	61
5.4 Hybrid positioning results	62
Conclusions	64
References	66
ANNEX 1: MicroStrain 3DM-GX2 specifications	68

1 Introduction

Global Positioning System (GPS) provides free positioning services for users around the world. This quality of the satellite navigation service will be further improved by the advances in receiver development and deployment of new sophisticated satellite signals. Moreover, within a decade, European Union and European Space Agency will declare another Global Navigation Satellite System (GNSS) called Galileo to be operational. Despite these improvements, satellite based positioning will not be realistic solution for deep indoors spaces where weak satellite signals face increasing attenuation due to building structures and signal degradation due to multipath propagation. Therefore, alternative solutions need to be deployed to establish indoor positioning system.

Indoor positioning can be based on existing infrastructure, specific equipment or a combination of these two. Existing positioning infrastructure can be e.g. cellular network [3]-[5] or network of base stations broadcasting commercial TV signals [6]. Specific equipment may contain a set of pseudolites forming a miniature ‘satellite navigation system’, an inertial sensor attached to a person’s shoe or a set of readers identifying specially designed tags based on RFID, IR, UWB, Zigbee, ultrasound or laser technology. There are tens of RTLS solutions in the market which can be used to track people and assets. In general, each of the solutions has its own advantages and limitations and thus, there is no single solution meeting all the needs.

Three positioning techniques suitable for indoor positioning in an industrial environment were selected for more detailed evaluation:

- WLAN location fingerprinting,
- Pseudolites, and
- Inertial navigation.

VTT’s own database correlation method (DCM) was used to represent WLAN signal strength based positioning methods. Ekahau, for instance, has a corresponding commercial product [7], but since previous tests with Ekahau’s WLAN positioning method indicate that the systems are comparable, using VTT’s method was considered more practical for the research and application development. It was also known that WLAN signal strength based positioning gets more inaccurate in large open areas. On the other hand, pseudolite system requires line-of-sight between 3-4 transmitters and the receiver. Therefore, a logical solution was to use pseudolite system in large open areas and use WLAN positioning as a supporting method to provide coverage elsewhere. The third positioning method selected for the evaluation, inertial navigation, doesn’t require any prebuilt infrastructure. It is used to track a pedestrian’s relative movement with the help of shoe-mounted sensor. Since the method can be easily combined with other solutions providing absolute position updates, it was selected to be used in the trial.

In the second year of the project a hybrid positioning solution was implemented. It utilizes marker-less vision based tracking to get absolute position fixes that can be used to aid Pedestrian Dead Reckoning (PDR). The idea of marker-less vision based tracking is to find corresponding features in current camera view and in images collected earlier from the environment. During the image database collection phase, location information and WLAN signal level data is assigned for each of the images. During positioning phase, WLAN positioning is used to limit the image database search and lower the risk of finding ambiguous image matches.

In the following chapter, theory behind the evaluated techniques is presented. Results from the pre-trials and two paper mill trials are described in chapters 3, 4 and 5 accordingly. The limitations of different positioning solutions and the accuracy requirements for different use cases are analysed.

2 Evaluated positioning methods and theory

2.1 WLAN signal strength based positioning indoors

WLAN signal strength based positioning methods can be divided into two categories. One uses signal propagation modelling and information about the building geometry and materials to convert the received signal strength measurements into distances between the mobile unit (MU) and transmitting access points. By knowing the access point locations and using trilateration, the location of the MU can be solved. The other category of WLAN signal strength based positioning is known as location fingerprinting. The idea of location fingerprinting is to create a database of reference fingerprints from the area in which MUs are to be located. The reference fingerprints are location tagged series of WLAN scans, which contain signal strength information from the detected access points. The positioning is conducted by comparing the signal strength information, measured by MU, to the signal strength information of the reference fingerprints and returning the location of the best matching reference fingerprint. The drawback of location fingerprinting methods is that changes in radio propagation environment caused by e.g. large, movable objects or AP transmission power adjustment will deteriorate the reference fingerprint database. As a result, the reference fingerprint database needs to be updated after changes are detected in the propagation environment.

2.1.1 Database Correlation Method

The Database Correlation Method (DCM) is a deterministic location fingerprinting method [3]-[5]. The DCM algorithm requires a measured or predicted reference fingerprint database. Each reference fingerprint is an average of several scans (typically 30) collected at the same location from all directions. The reference fingerprint grid is usually non-uniform and sparse simply because building walls, furniture and other objects limit the area where measurements can be done. This is taken into account in the position estimation process by utilizing multiple best matching fingerprints locations. The location of the MU is then calculated as a weighted average location of the best matching reference fingerprints. DCM includes also a penalty term that penalises reference fingerprints that do not contain all the access points that are detected by the MU [4].

2.2 Pseudolite positioning

Pseudolites (pseudo satellites) are ground based transmitters that generate and transmit GPS-like signals. The main factor that limits the use of GPS is the requirement for line-of-sight between the satellites and the receiver antenna. Pseudolites can be installed to improve availability and accuracy of GPS based positioning in locations that have poor satellite visibility like urban canyons, valleys, and deep open pit mines. Indoors where the GPS signals are heavily attenuated, a set of pseudolites can be even used to replace the whole GPS constellation.

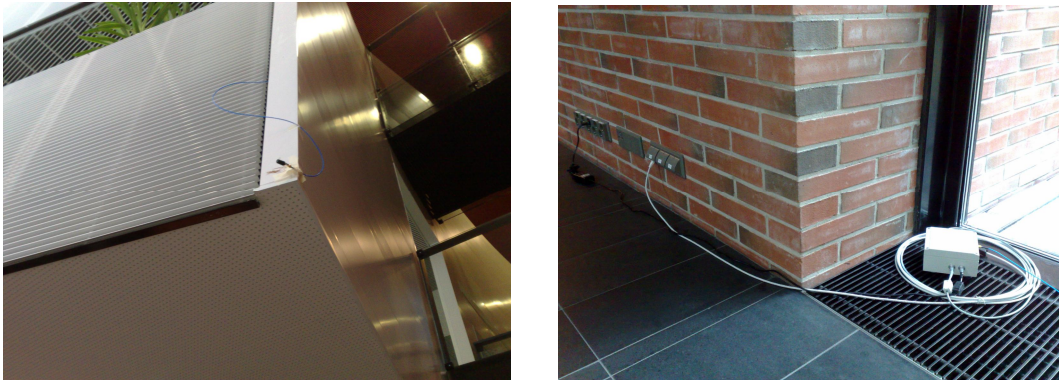


Figure 1. Space Systems Finland's pseudolite antenna and signal generator used in indoor positioning trials.

Pseudolites have several benefits compared to a pure satellite based system. First of all they can improve the availability of the GPS system. The number and locations of the pseudolites can be adjusted according to the environment to improve both the vertical and horizontal dilution of precision (DOP) and thus, to maximize the accuracy and the performance of the system [9][10][11]. Moreover, as being ground based transmitters, pseudolites are not affected by the ionosphere, which is the major source of error in GPS based positioning [9]. Because they can operate on the same frequency as GPS, they can be deployed to the standard GPS receiver with only minor modifications to the firmware [12]. In indoor case, the aim is to provide seamless outdoor-indoor positioning using the same receiver equipment [11].

Augmented GPS or pure pseudolite constellations have been used e.g. in aircraft landing [13], land vehicle navigation in urban environments [11], deformation monitoring systems [9], precision approach applications and Mars exploration [14]. Pseudolites are mainly used in places where real-time positioning at centimetre-level is required. Automating the heavy and expensive mining machines in open-pit mining has been one of the major applications [15].

2.2.1 Pseudolite positioning systems

Pseudolite positioning systems may vary a bit in details. The text later follows mainly specifications of the Space Systems Finland's (SSF) pseudolite system, which was used in the trials.

SSF's pseudolite positioning system consists of pseudolite signal generators, transmission antennas, a firmware-modified reference GPS receiver, a firmware-modified user GPS receiver and a master control station (MCS). The overview of the system is depicted in the following Figure 2.

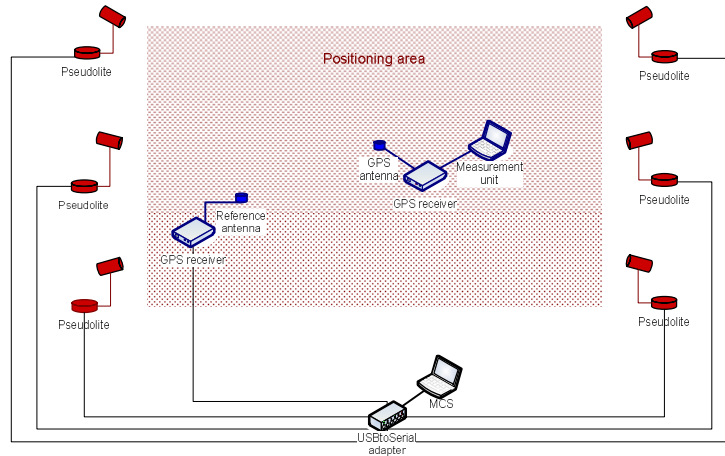


Figure 2.Overview of the SSF's pseudolite positioning system.

Transmission antennas are connected to signal generators with antenna cables and each signal generator is connected to the MCS with a serial line connection or radio link. The MCS is used to control the pseudolite network. It gathers measurement data from the reference GPS receiver and handles the synchronization of the pseudolites (see chapter 2.2.2).

A pseudolite signal generator generates GPS-like L1 carrier signal (frequency 1575.42 MHz) and modulates it (50 bits/s) with the C/A code and navigation signal [17]. The C/A code is the same as used in GPS satellites [16]. The navigation signal is provided by the MCS via serial line connection). The MCS is also used to set the PRN (pseudo-random noise) numbers used and to control the signal strength of the signal generators.

In most cases, two kinds of transmission antennas are used in pseudolite systems: small and large helix antennas. The small helix antenna which has a wider antenna pattern is generally used attached to the centre of the ceiling. The large helix antenna which has a narrower antenna pattern is used in corners where the ceiling and walls might cause reflections. It is also suitable for problematic areas because its antenna pattern is better controllable by adjusting the length of the helix [16].

As GPS receivers, pseudolite systems use normal outdoor GPS receivers. However, firmware modifications are needed to both the reference receiver and the receiver used for navigation. At the moment, standardization of the pseudolite systems and the GPS receivers is not progressing towards augmentation with pseudolites. The objective to use any kind of GPS receivers (e.g. built in to mobile phones) both in GPS, augmented GPS and indoor navigation don't seem to be achieved in the near future.

2.2.2 Synchronization

In an augmented GPS system, the synchronization is done to GPS time. In a pure indoor composition either one of the pseudolites is selected as a master pseudolite, in relation to which the rest of the pseudolites are synchronized (like in SSF's case), or the synchronization is done to a master station.

The synchronization of the pseudolite system is based on pseudorange measurements. The reference GPS receiver tracks the pseudolite signals and sends measurement reports to the MCS. According to the measurements MCS adjusts the pseudolite signals so that their range measurements match the geographical distance between pseudolite and reference receiver. The signal adjustments are done in three phases: first the frequency of the pseudolite signal is

adjusted, then code synchronization is performed and finally fine adjustments are made according to the carrier phase. Based on the synchronization results the pseudolites provide correction messages to the navigation unit.

2.2.3 Known weaknesses

Indoor navigation with pseudolites has some practical problems [10], such as:

- near-far problem,
- unknown transmission position,
- time-tag, and
- multipath problems.

The near-far problem is caused by the variation in the received signal power of the pseudolites when the distance between the receiver and the transmitters changes. A pseudolite in the vicinity of receiver may overwhelm the signals from other pseudolites/satellites and jam the receiver. On the other hand, if some of the pseudolites reside too far away, their signal level may be too weak to allow the receiver to detect them. Transmitting the pseudolite signal in short pulses with a low duty cycle can be used to minimize the effect of the near-far problem [13].

To set up a pseudolite system, the accurate locations of the transmitters have to be measured and defined. This can be a challenging task especially if the system is planned to be built quickly or in a place where there is no other way to define locations than measuring distances from a known location (e.g. in indoor spaces and drift mines). In publications, some methods to calibrate pseudolite positions have been represented [10].

Pseudolite signal generators are usually equipped with low-cost crystal clocks in order to reduce their unit price while the GPS satellite uses an atomic clock. These inaccurate clocks drift and therefore decrease the positioning accuracy. This problem is overcome by deploying a master station that has more precise clock. The master station will keep the pseudolites in time by sending synchronization messages to them [9]. In indoor navigation, an alternative approach is to synchronize pseudolites to a master pseudolite. Asynchronous pseudolites have also been used indoors [16].

Multipath propagation of the signal deteriorates the accuracy especially in an environment having plenty of reflecting surfaces and diffracting edges [12]. The problem is very significant indoors where many reflecting materials are used and where the elevation angle from the receiver to the pseudolite transmitter is small [9]. The multipath problem can be reduced by using transmitter and receiver antennas with controlled antenna patterns. The transmitter antenna itself can cause multipath propagation, so selecting the antenna positions is also important.

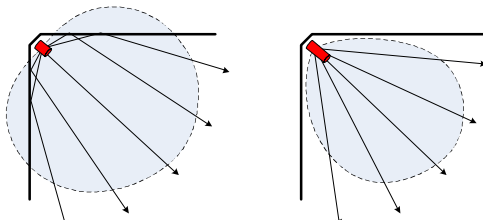


Figure 3. Multipath effect caused by an antenna (left) and antenna which reduces it.

It should also be noted that if pseudolites are e.g. transmitting L1 signal, they can jam real GPS L1 signals, denying GPS service to nearby receivers that are not configured to measure signals transmitted by pseudolites [12]. The problem can be solved by using pulsed signals.

2.3 Inertial/magnetic sensor positioning

Inertial sensors, i.e. a combination of accelerometers and gyroscopes, are used for dead reckoning. Dead reckoning refers to the process of determining a position relative to an earlier known position by using information about the velocity, the course, and the elapsed time. Gyroscopes measure the angular velocity in the sensor frame. Accelerometers measure the sensed acceleration, which is a sum of Earth's gravity and the specific force acceleration caused by the linear movement of the sensor. By combining this information to get the sensor attitude (rotational motion) and the travelled distance (translational motion) the relative movement in the Earth coordinate frame can be followed.

Magnetic sensors are used as electronic compasses; thereby they provide the heading of the sensor relative to Earth's Magnetic North Pole. Unfortunately, the accuracy of this heading information is compromised by various electrical and environmental sources. In addition to sensor based errors caused e.g. by sensor misalignment and temperature changes, the error sources include hard iron and soft iron field distortion. The presence of a magnetized object and permanent magnetized fields (e.g. from electrical currents) create a constant magnetic bias on the electronic compass output. This is called hard iron distortion. Soft iron distortion creates an orientation-dependant magnetic bias to the sensor output. Soft iron effects are caused by ferromagnetic materials that generate magnetic fields in response to externally applied fields. Indoors, metallic building structures cause soft iron field distortions. Electric equipment and power lines cause hard iron field distortions. Soft and hard iron effects that are moving with the sensor (and the pedestrian) may be compensated, whereas effects from the environment can only be detected and not removed. Due to these error sources, the use of electronic compass in heading estimation becomes much more difficult indoors than outdoors.

IMU (Inertial Measurement Units) is a wider term for a system including several integrated navigation aids: e.g. MEMS (microelectronic mechanical system) accelerometers, MEMS gyroscopes, magnetometers, possibly also barometers, GPS, sonar, or radar.

2.3.1 INS mechanization

For calculating the position and velocity based on the acceleration sensed by the accelerometer, the standard strapdown INS mechanization equations need to estimate the attitude of the sensor. This is done usually by updating a rotation matrix with detected attitude changes sensed by a gyroscope. A rotation matrix R_b^n can be used to transform sensor frame acceleration vectors to the navigation frame. The attitude update is done by multiplying the R_b^n by a matrix R_b^{b-1} which is formed based on angular rate changes sensed by the gyroscope. Alternatively a quaternion based approach can be used. After this the sensed linear acceleration is converted to navigation frame and double integrated to get the relative position.

2.3.2 ZUPT based Pedestrian Dead Reckoning (PDR)

As mentioned earlier, in standard strapdown INS mechanization, travelled distance is calculated by double integrating the acceleration sensed by the accelerometer. However, even a tiny drift rate of the used gyroscope causes a slowly increasing tilt error. Furthermore, this

tilt error causes horizontal acceleration error equal to 9.8 m/s^2 times the tilt error in radians [22]. Therefore, it is impossible to track movement of a pedestrian for more than a few seconds using the standard strapdown INS mechanization alone.

Gait sequence can be divided into two phases; a stance phase and a stride/swing phase. When the sensor is attached to the foot, the stance phase can be detected. By assuming that the velocity is close to zero during the stance phase, the increasing tilt error can be corrected after each stride phase. This method is called the Zero velocity update (ZUPT) technique.

The ZUPT algorithm applied in the NOSE is developed based on [22] where a complementary form of EKF (Extended Kalman Filter) was used to track 15 error parameters (three dimensional attitude errors, gyro biases, position errors, velocity errors, acceleration biases). By using these error estimates in strapdown INS mechanization, it is possible correct the tilt error and estimate travelled distance based on the specific force acceleration caused by the foot movements. ZUPT lets the EKF correct position, velocity, accelerometer biases, pitch, roll and the pitch and roll gyro biases. Heading and the heading gyro bias are the only states in the complementary EKF which are not observable from zero-velocity measurements [22]. However, heading correction can be introduced to the system by using electronic compass which senses the Earth's gravitational field.

2.3.3 Alternative solutions for PDR

A commonly used approach for Pedestrian Dead Reckoning is to use the accelerometer for step detection and step counting [23]. The step detection can also be made based on magnetometer outputs [24]. Step detection can be based on zero crossing, autocorrelation or peak detection method [23]. By assuming simply a constant step length, the travelled distance can be estimated. The drawback of the method is that it cannot directly detect the direction of the movement. Thus, every time when a step is detected, it is assumed that the user moves forward. Gyroscope and electronic compass is often used to track the changes in the sensor heading.

PDR can be further improved by performing step length estimation by using predetermined relationship between step length and step frequency. However, this relation cannot be uniformly modelled for all the types of movement (slow walk, fast walk, jogging, running etc.). The relationship is also dependant of the user's individual walking style. Therefore, personal calibration can be used to improve the estimation.

The step detection/step length estimation based PDR can be improved even further by estimating the movement direction via Principal Component Analysis (PCA) of the specific force acceleration caused by walking motion. The gravitation-free acceleration vector is projected onto the horizontal plane perpendicular to the direction of gravitation. The resulting residual vector represents the total horizontal acceleration. By applying PCA to the time series for the horizontal acceleration vector, the axis for the forward-and-backward direction can be estimated [27].

2.4 Methods for data fusion and filtering

The Kalman filter is a recursive solution of the discrete-data linear filtering problem. The word recursive means that the filter uses the information about its previous state during the estimation process of the current state. Solving the location of a user based on positioning measurements (provided by DCM or other method) is non-linear state estimation problem and

therefore, Kalman filter is not optimal filtering technique for that. In Extended Kalman filter (EKF), the non-linear transition function is linearized by calculating a matrix of partial derivatives (the Jacobian) of the state transition function. This enables the filter to be used in positioning.

Particle filtering is a technique that implements a recursive Bayesian filter using the Sequential Monte-Carlo (SMC) method. It consists of a set of random samples called particles. When applied to positioning, these particles represent the probability density function (PDF) of the user location.

In the evaluated Particle Filter, the movement of the particles is based on relative positioning information provided by the complementary EKF introduced in 2.3.2. Weights of the particles are calculated based on the particles' distance to the latest DCM location estimates similarly to [28]. The particles' movement is also limited using the technique called Map Filtering [29]. In Map Filtering, digital floor plan is used to restrict particles' movement so that they cannot cross through walls or other building structures. The weight of a particle that crosses illegal area is set to zero. Re-sampling of the particles is performed to guarantee that particles moving to a wrong direction (having low weight) and particles hitting walls (having zero weight) are relocated in an area where the user most likely resides. At the beginning of a measurement, particles are created around the first DCM estimate forming 2D Gaussian distribution with standard deviation of 3 meters.

2.5 Hybrid positioning utilizing marker-less vision based tracking

Marker-less vision based tracking compares current view detected e.g. by a web camera with reference images collected earlier from the environment. During the reference image collection, location data is assigned for each of the images. In the positioning phase, if the current camera view has enough similarities with one of the reference images, the location of the camera (and user) can be estimated to be equal with the location of the best matching reference image. As an example, Figure 4 depicts corresponding features between two images with green lines.

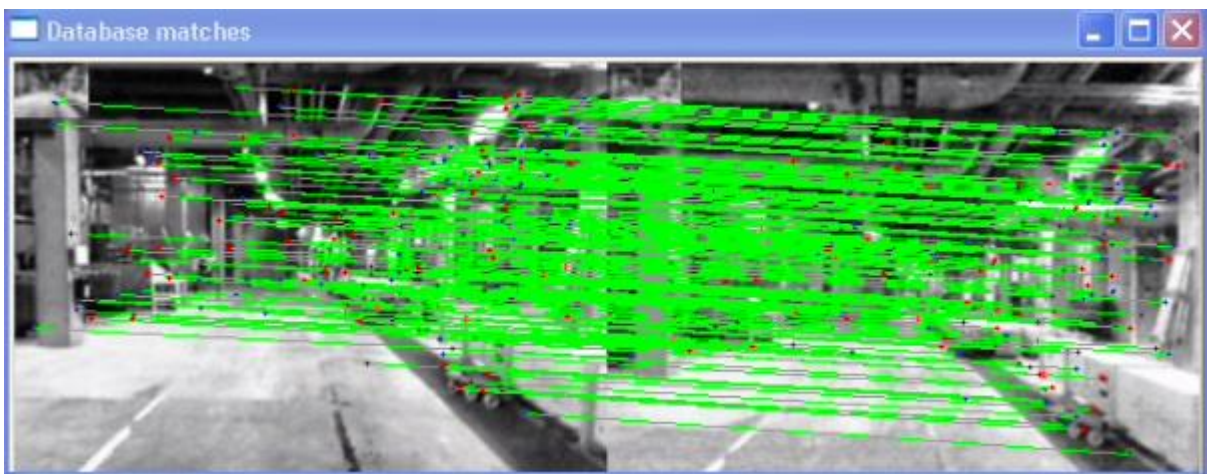


Figure 4. Green lines show the corresponding features between current camera view (left) and best matching reference image.

Marker-less tracking alone is prone to yield false image matches if there are ambiguities in the environment. For instance, similar looking corridors can be found in many parts of a building.

Moreover, reference image database for one building may consist of thousands of images, so the comparison process becomes quickly too burdensome unless the search space is somehow limited. Coarse WLAN positioning based on signal level data of strongest detected access points provides means to limit the user location with 5-20m accuracy. If the signal level data is collected along with the image database, the deployment of the method does not require any additional work or knowledge about the access point locations. Thus WLAN positioning is well suited for making marker-less tracking less prone to errors and better scalable to large buildings.

If the use case for the indoor positioning requires continuous location updates to be available, marker-less vision based tracking can be combined with strap-down inertial navigation (for shoe-mounted sensor) or step detection + step length estimation in case of waist-mounted sensor. These techniques can be combined e.g. by using a Kalman filter which estimates the state including position and heading. As a result, the location of the user can be continuously tracked even if marker-less tracking does not detect any matches for a long period of time. Moreover, with this hybrid approach the user can also be positioned in areas from where there are not reference images taken.

3 Pre-trials

The main pilot for pedestrian navigation was carried out in Kvarnsveden paper mill in September 2008. In order to test the equipment and to develop software components and algorithms two preliminary trials were done in VTT's buildings. The pilot and the pre-trials included measurements with three different positioning methods: pseudolites, WLAN location fingerprinting, and inertial sensors. First tests were carried out in Digitalo. The measurements were done in co-operation with VTT's own HYPEL project.

3.1 Digitalo pre-trial

3.1.1 Trial area

Digitalo represents a typical modern office environment. It is built with wings of office rooms and open plan offices around an open square in three floors. The skeletal structure is made of concrete and steel, the outer facade is brick and low emissive glass. Glass is also common interior material as plasterboard and concrete. The main hall is quite low (about 3 m) and its ceiling has unusual forms (see the white ceiling structure in the first picture).

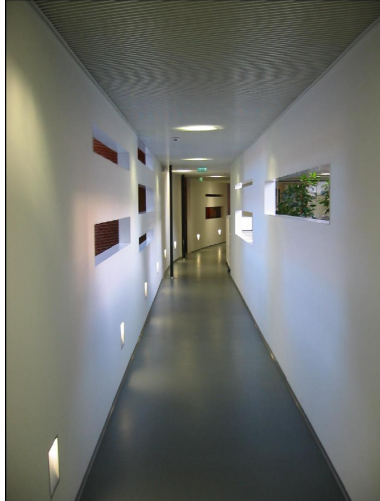


Figure 5. Pictures from Digitalo. The entrance hall and cafeteria (uppermost), corridor above it (down left and down in the middle), and an office environment (down right).

3.1.2 Trial setup

In NOSE project, in spring 2008, Digitalo's WLAN network was changed to better match the indoor positioning needs. Five new WLAN access points were added to the network so that in trial altogether 31 Cisco's WLAN access points were placed in three floors. 11 APs were set into the ceiling structure in the first floor (see Figure 6) and the rest of the APs were evenly distributed to the wings of the other two floors.

In June 2008, the pseudolite positioning system was built using Space Systems Finland's pseudolites and antennas. The following devices were used:

- Six pseudolites
- Five Sarantel helix antennas and one large helix antenna
- A laptop as a Master Control Station (MCS) running Linux Ubuntu (kernel 2.6.22-14) and SSF's server software
- Fastrax iTrax03EvaluationKit GPS receiver as a reference receiver running SSF's software

- Edgeport 8 port USBtoSerial adapter
- CAT6 cabling

Another Fastrax iTrax03EvaluationKit GPS receiver was used for navigation and positioning measurements. The firmware was modified by SSF.

The pseudolites were placed around the main hall as depicted in the following Figure 6.

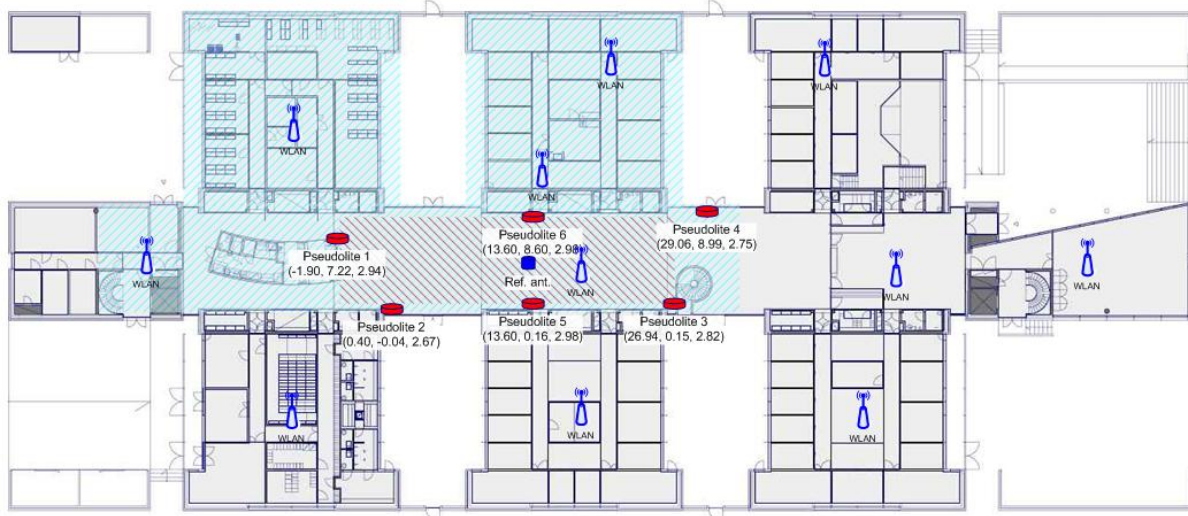


Figure 6. Digitalo trial setup. Pseudolite antennas (red symbols) and WLAN access points (blue symbols) with pseudolite (dark red hatched) and WLAN (light blue hatched) trial areas.

Pseudolite antennas were attached on the ceiling and wall structures at the same altitude than the lowest ceiling structure in the middle of the hall. Each pseudolites were connected to the master control station via Erve network cabling and the USBtoSerial adapter. The reference receiver was connected directly to the MCS with a null modem cable. The antenna of the reference receiver was placed on a table in the middle of the trial area. For positioning, a local coordinate system was created. The coordinates of the pseudolites and the reference antenna were measured using a plumb line and a laser distance-meter.

In the following, some pictures from the Digitalo setup are shown.



Figure 7. Pseudolite number 1.



Figure 8. Pseudolites number 5 (left) and 4 (right).

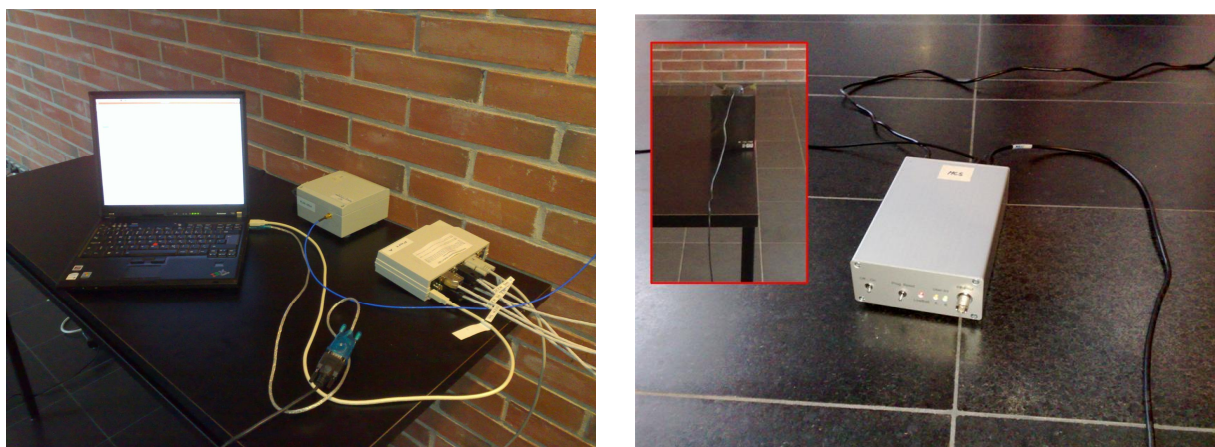


Figure 9. MCS laptop and Fastrax reference receiver.

An IMU (Microstrain 3DM-2GX), consisting of 3-axis gyros, accelerometers, and magnetometers was attached tightly to the right shoe of the pedestrian as shown in Figure 10. See Annex 1 for details and specs of the sensor system.



Figure 10. IMU (Microstrain 3DM-2GX) attached to a shoe.

3.1.3 Pseudolite measurement results

For discovering the pseudolite system performance, the operating range of the configuration was checked. 27 reference points (RPs) (see Figure 15) were used to collect static measurement data. The measurement unit was manually initialized at RP26, then the receiver was moved to the next RP and approximately 60 position estimates were collected for every RP. If the border of the operating range was reached at some point, the measurement unit was manually initialized again at RP26 in order to proceed with the remaining RPs. The sampling rate was 1Hz and all the pseudolites were synchronized in continuous signal mode. The six pseudolites were mapped to PRN numbers according to the Table 1.

Table 1. Pseudolite PRN mapping.

Pseudolite number	PRN number
Pseudolite 1	PRN60
Pseudolite 2	PRN61
Pseudolite 3	PRN62
Pseudolite 4	PRN63
Pseudolite 5	PRN64
Pseudolite 6	PRN65

The position estimates collected at a single RP, e.g. RP25, were plotted (Figure 11) and analyzed to find out the following details: the number of pseudolites used for the position fix (Figure 12), what is the relation between the estimated error and the actual error (Figure 13) and whether the fix is considered reliable or not by the pseudolite position system (Figure 14). Moreover, the mean position based on all the estimates and the standard deviation of the position estimates for both X and Y axes were calculated. Finally, the positioning error between the mean position estimate and the actual location (i.e. the RP under consideration) was also calculated.

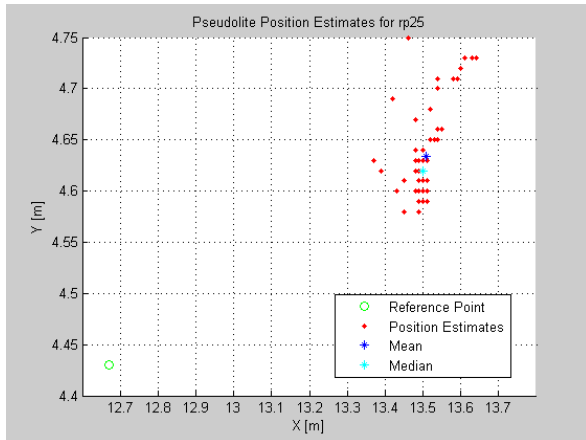


Figure 11. RP25 position estimates.

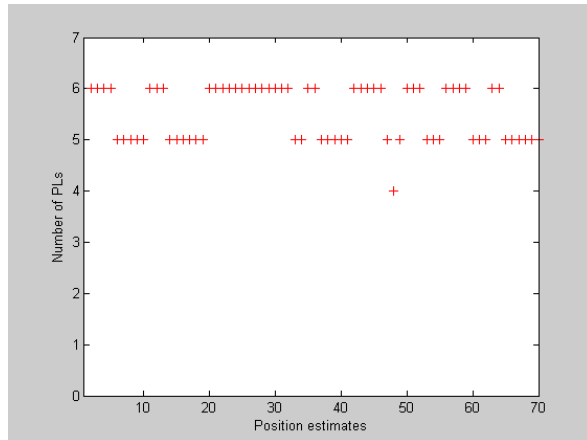


Figure 12. Number of pseudolites used in RP25.

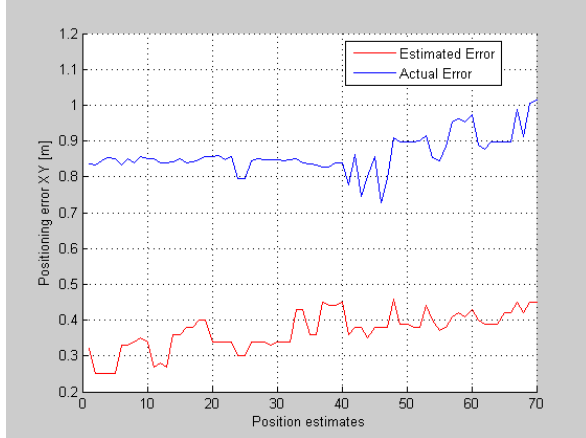


Figure 13. Comparison of estimated and actual errors.

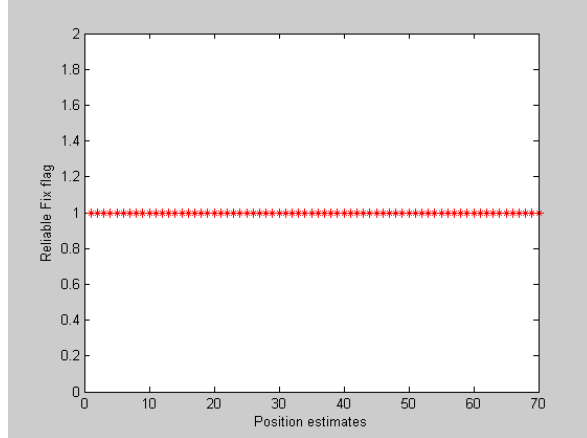


Figure 14. A flag telling whether the fix was considered reliable.

For RP25, the standard deviation was about 4 cm in both axes and the positioning error was 0.86 m. Results from all the reference point measurements are shown more detailed in the following table. Number of pseudolites used for the position estimate, information whether the estimate was considered reliable or not by the system and the actual positioning error are listed for each reference point. It should be noted that usually if the fix was considered unreliable, the measurement unit was too close to a pseudolite (near-problem) and the system returned the coordinates of that pseudolite as the position estimate. In those cases, the PRN number(s) are included in the table, instead of the positioning error.

Table 2. Reference point measurement results.

RP11	4 PLs Unreliable fix PRN60	RP21	4 PLs Unreliable fix PRN60	RP31	3 PLs Unreliable fix PRN60, 62
RP12	4 PLs Unreliable fix PRN60, 64, 65	RP22	3-5 PLs Unreliable fix 6.4m	RP32	3-5 PLs Mostly unreliable fix 1.4m
RP13	3-5 PLs Reliable fix 2.7m	RP23	3-5 PLs Reliable fix 4.6m	RP33	5 PLs Reliable fix 3.5
RP14	4-6 PLs Reliable fix 1.9m	RP24	4-5 PLs Reliable fix 2.6m	RP34	5-6 PLs Reliable fix 1.1m

RP15	4-5 PLs Reliable fix 0.83m	RP25	5-6 PLs Reliable fix 0.86m	RP35¹	3 PLs Unreliable fix PRN65
RP16	3-4 PLs Reliable fix 1.4m	RP26	5-6 PLs Reliable fix 0.02m	RP36	4-6 PLs Reliable fix 1.5m
RP17	3-5 PLs Reliable fix 3.2m	RP27	4-5 PLs Reliable fix 0.66m	RP37	5-6 PLs Reliable fix 1m
RP18	4 PLs Unreliable fix PRN62, 63, 64	RP28²	3 PLs Unreliable fix PRN63	RP38³	3 PLs Unreliable fix PRN62, 63
RP19	4 PLs Unreliable fix PRN62, 63, 64	RP29	4 PLs Unreliable fix PRN63	RP39	3 PLs Unreliable fix PRN63

The area in which positioning was feasible and the fix was considered reliable (“coverage area”) is depicted in the Figure 15 with green colour. Using continuous signals, positioning was feasible in a rectangular 78m² area shown in Figure 15, with the exception of RP35 when the user was close to pseudolite number 6. Positioning accuracy was below 3.2m in the rectangular 60m² area (RP14, RP34, RP37, RP17), with the exception of RP35. The position estimates had small variance and they suffered mostly by a bias error which was greater when the measurer moved away from the initialization point. The estimated positioning error provided by the pseudolite system underestimated the actual positioning error (except for RP26, which is the manual initialization point) when the measurer moved towards the cafeteria (to the left in the Figure 15) and overestimated the actual positioning error when the measurer moved towards the entrance (to the right in the Figure 15).



Figure 15. Reference points used to collect position estimates. Green colour shows the best operating range of the pseudolite position system using continuous signals, yellow a bit problematic areas and red the areas where reliable position estimates couldn't be

Static measurements with pulsed signals were also performed. However, two of the pseudolites couldn't be synchronized in RTCM mode due to the differences in signal generators. Thus, those two pseudolites were kept all the time in continuous mode. In Digitalo, only small differences between measurements made using continuous and pulsed signal mode were seen. The coverage area was slightly larger as it was expected to be, but in route measurements the results were worse than expected.

¹ Data collected for RP35 in another test reveal that there is mostly reliable fix, 3-6 PLs are used and the positioning error is 2m.

² Data collected for RP28 in another test reveal that there is always reliable fix, 4-5 PLs are mostly used and the positioning error is 2m.

³ Data collected for RP38 in another test reveal that there is always reliable fix, 4-5 PLs are mostly used and the positioning error is 1.7m.

Position estimates were also collected by moving with fixed velocity along different routes. In the measurements either continuous signals or pulsed signals (RTCM) were used. The system was synchronized so that SNRs for the pseudolites were with the continuous signals in the ranges of 42-43 (PRN60-63) and 45-48 (PRN64-65) and with the pulsed signals in the ranges of 40-44 (all). The measurement unit was manually initialized at a reference point previously chosen and different routes inside the “coverage area” were recorded. (In most cases the initialization point was RP26.) Each route was sampled two or three times (Route a, b and c) in order to investigate the consistency of the pseudolite positioning system. In some measurements, the route ended outside the best positioning area. For the last set of the measurements, the trial area was cleared of all the tables to find out the effect of the furniture in the system performance and be able to move around more freely.

“Real life” measurements without manually initializing the starting point were also performed but the results were unsatisfying - mainly because relatively good first fixes were hard to get in a reasonable time. When positioning with carrier phase data, the initial position error plays a critical role [20]. It affects to the position estimates far along the measurement. If the first position estimate is totally wrong then it is hard to see how the system behaves and what are the effects caused by the environment. In Digitalo, all the route measurements were decided to do with manual initialization which is not always acceptable in real scenarios but gives more information.

Route T5_1a-c was a direct route where 8.2 meter distance were walked towards the cafeteria (from right to left in the Figure 16) and back starting from the RP26. Mostly 4-5 pseudolites were available for each position fix. As a result, the estimated route was different in all three measurements but they have some similar characteristics. The position estimates are biased in the Y coordinate and in the X coordinate they do not reflect the length of the actual route. Measurement b gave the best results, but still there is some bias in the Y axis, which is very strong for the last estimates.

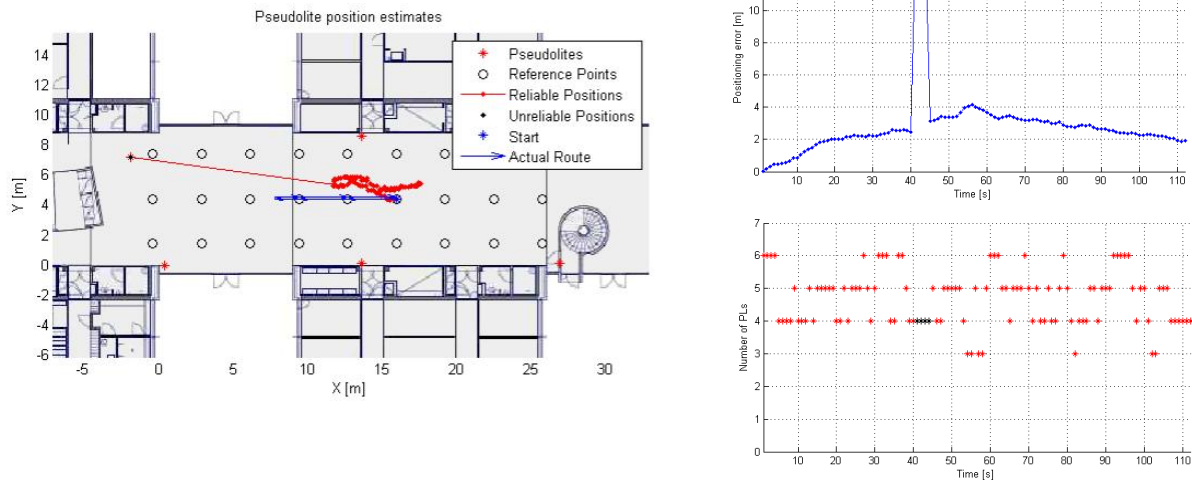


Figure 16. Route T5_1a.

For Route T5_2 mostly more than 4 pseudolites were used for position fix. It's seen in all three measurements that the system couldn't provide accurate estimates. The same characteristics as in the previous route can be seen. The estimates are biased in the Y coordinate and in the X coordinate they do not reflect the length of the actual route.

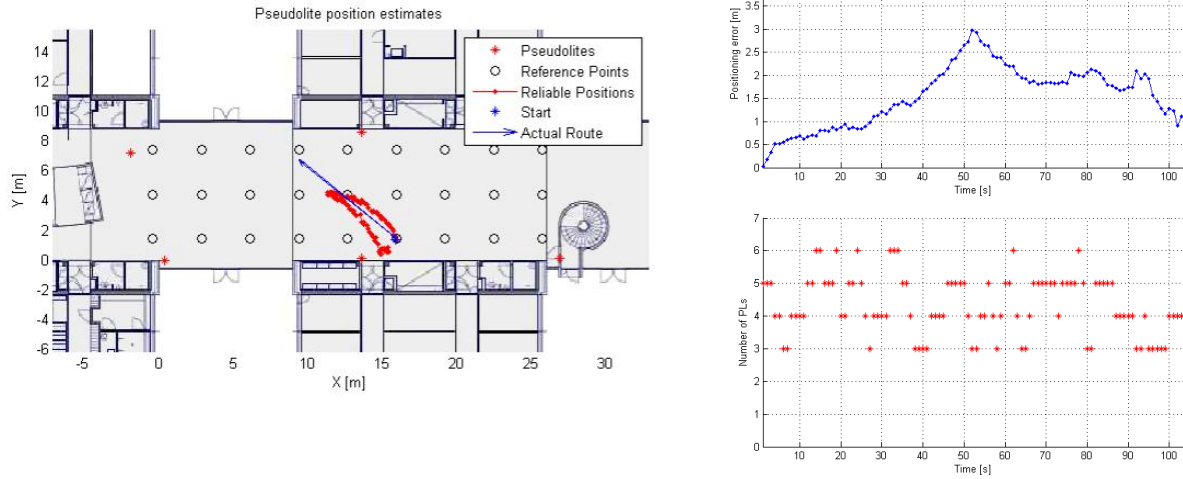


Figure 17. Route T5_2a.

In the following figures, some results measured using both continuous signals and pulsed signals are presented. The pulsed signal didn't improve the results unlike was expected. In RTCM mode more cycle slips were detected. In Route T3B_5a, tracking was good at the beginning but then the position estimates were shifted towards PRN64 deviating from the actual path. Moreover, the last part of the route is shifted up close to PRN65. In Route T3B_5b, tracking was good until the middle of the route and then the position estimates were heavily affected by PRN64 and didn't reflect the actual route.

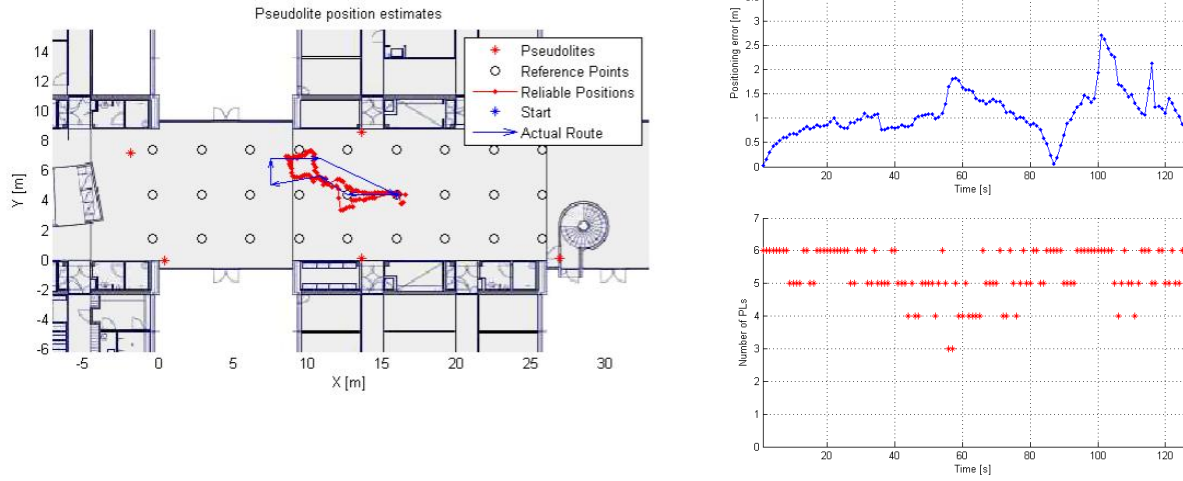


Figure 18. Route T2A_5b with continuous signal.

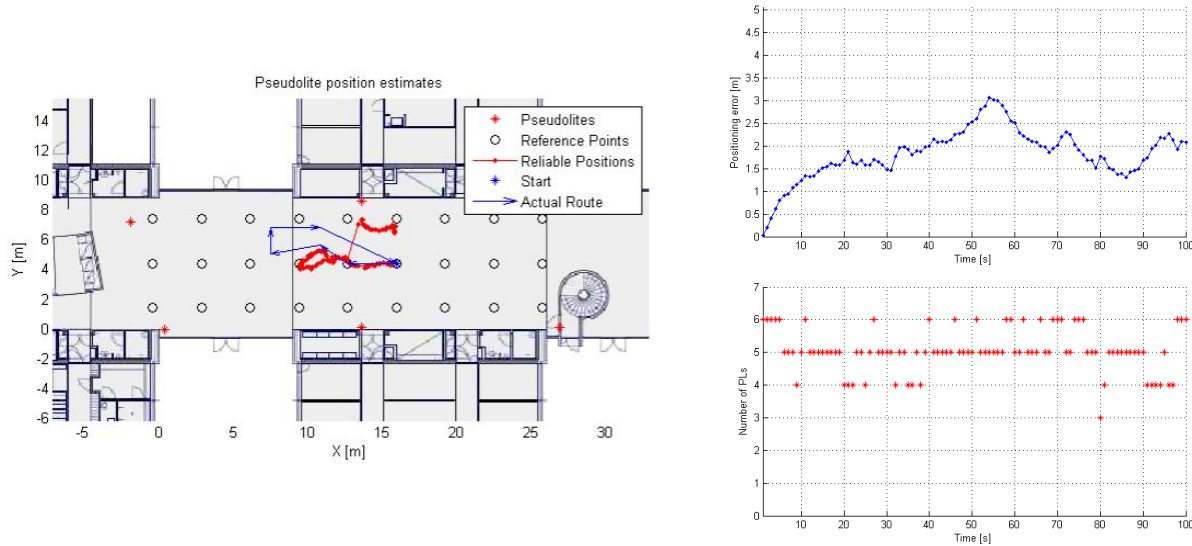


Figure 19. Route 3B_5a with pulsed signals.

The positioning errors from the selected routes are presented in the following table.

Table 3. Positioning errors of selected routes in Digitalo trial.

Route	Mean positioning error [m]	Standard deviation
Route T5_1a	2.817	1.985
Route T5_1b	1.671	0.976
Route T5_1c	1.250	0.655
Route T5_2a	1.554	0.664
Route T5_2b	2.277	1.110
Route T5_2c	1.379	0.773
Route T2A_1b	1.787	1.166
Route T3B_1b	1.281	0.888
Route T2A_5b	1.089	0.475
Route T3B_5a	1.826	0.557

In Digitalo, the system configuration wasn't consistent because of the propagation environment and some differences in pseudolite signal generators. During the synchronization process a slight modification of the attenuation levels for some pseudolites was usually required to achieve SNRs in the desired ranges. The pseudolite system could rarely find a fix at start-up, unless manual carrier initialization was used to provide the exact coordinates of the starting location.

All the measurement results were suffered from the same kind of constant bias error which was different depending on the direction of motion. The errors were most likely caused by the fact that the room was a bit low for pseudolite system and the LOS wasn't pure enough everywhere in the measurement area. The signals were also affected by strong reflections and diffractions from the ceiling. Estimated routes were different for the same actual route which tells about frequent cycle slips caused by the propagation environment. The same behaviour was also seen in reference point measurements. Starting from the same initialization point and then moving towards a reference point to collect static measurements, gave different accuracy results when different paths were followed to reach the reference point.

Although the main hall of Digitalo wasn't the most ideal environment for pseudolite system, some improvements can be made to get it operating better. E.g. reflections can be reduced by changing the setup and antennas. Some of the reflections were caused by the non-optimal antenna type and placement.

Because the pseudolite tests were unsatisfying in Digitalo, more tests with the pseudolite system were decided to do in more appropriate environment before the paper mill pilot.

3.1.4 WLAN location fingerprinting results

The accuracy of Database Correlation Method presented in 2.1.1 was evaluated using 285 reference fingerprints collected from all the three floors in Digitalo. Reference fingerprints were collected with Fujitsu-Siemens Pocket Loox smart phone. Dell D820 was used to collect RSS data along the test measurement route. RSS data was tagged with actual location information using Site Survey tool developed at IST-Motive project. The test route formed a winding path from front door on the 1st floor to 2nd floor office room. Total length of the route was ~210m. The route was repeated 5 times. In order to plot the results on top of a floor plan, the route was divided into two parts. For instance, route name D12 corresponds to the 1st floor part of the 2nd repeat of the route.

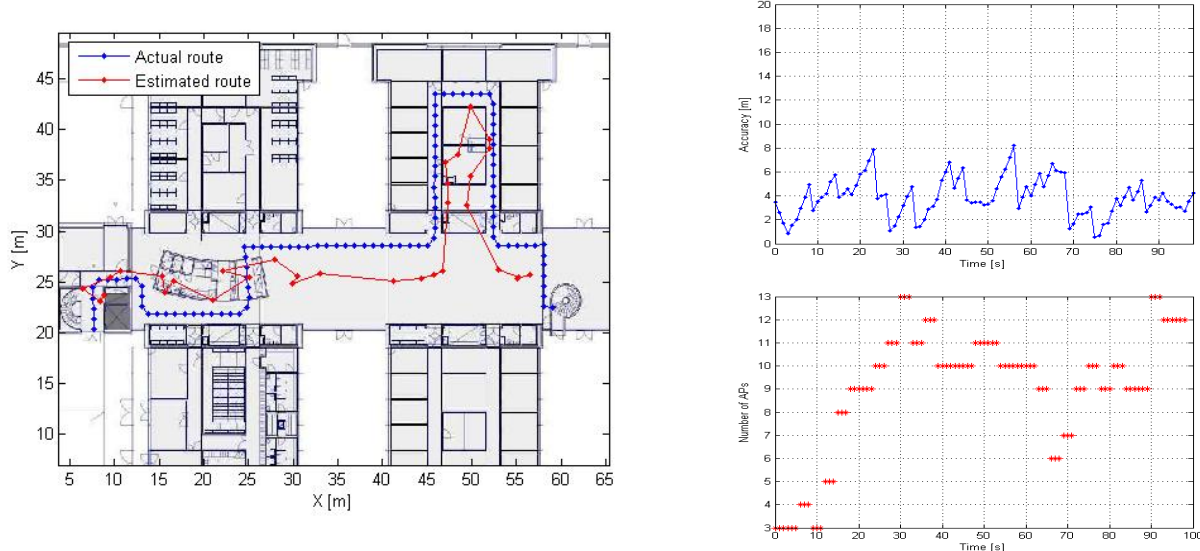


Figure 20. 1st floor part of the route positioned with DCM (1st repeat).

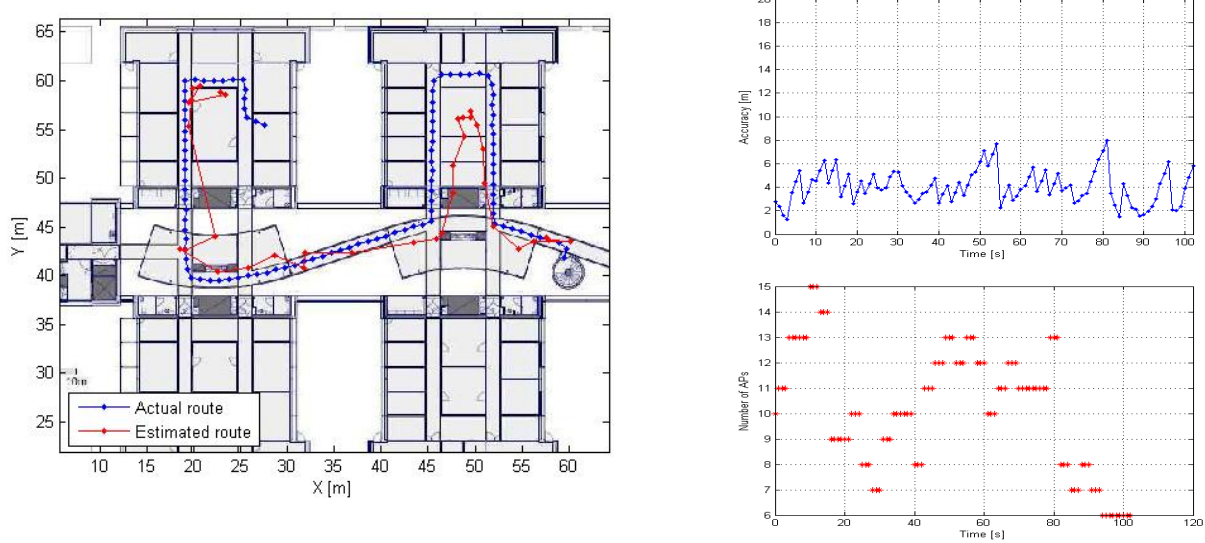


Figure 21. 2nd floor part of the route positioned with DCM (1st repeat).

The average accuracy using DCM is around 4m in both of the floors. As can be seen in Figure 20, the method is able to predict the shape of the route but fails distinguish the details of it. Maximum error occurs nearby the cafeteria in the central hall. Open areas like the central hall tend to disperse radio signals, leading to much less distinction among collected reference fingerprints, and therefore, to poorer positioning accuracy. Like on 1st floor, mean positioning accuracy is around 3-4 meters on 2nd floor part of the route. The first repeat of the 2nd floor part of the route is shown in Figure 21.

Numerical results from all five repeats are depicted in Table 4.

Table 4. DCM results from 1st and 2nd floor parts of the route repeated 5 times.

Route:	Samples:	Mean [m]:	CEP 50% [m]:	CEP 67% [m]:	CEP 95% [m]:	Max error [m]:
D11	99	3.9	3.7	4.3	6.7	8.2
D12	99	3.8	3.8	4.4	6.6	7.3
D13	99	3.6	3.5	4.1	6.3	7.3
D14	99	3.9	3.9	4.5	6.0	7.7
D15	99	3.9	3.9	4.4	6.6	7.3
D21	103	4.0	4.0	4.5	6.4	8.0
D22	103	3.8	3.8	4.6	6.6	7.6
D23	103	3.5	3.4	4.2	7.0	9.3
D24	103	3.8	3.6	4.4	7.2	8.4
D25	103	3.8	3.6	4.4	6.7	11.0

Afterwards it was noticed that the true scanning rate of the Dell D820 laptop WLAN card is lower than the expected 1 scan per second (it is around 1 scan per 3 seconds). The lower scanning rate most likely decreases the positioning accuracy of a moving user, because the signal strength information is not updated frequently enough.

Extended Kalman filter was tested to filter out the outlier DCM estimates and to predict the route shape more accurately. Since in most of the cases, DCM estimates contain more bias-like than noise-like errors, EKF yields only slightly better accuracy than DCM without

filtering. This is illustrated in Figure 22. However, EKF manages to filter out sudden jumps along the route and delivers more continuous trajectory of the walked path.

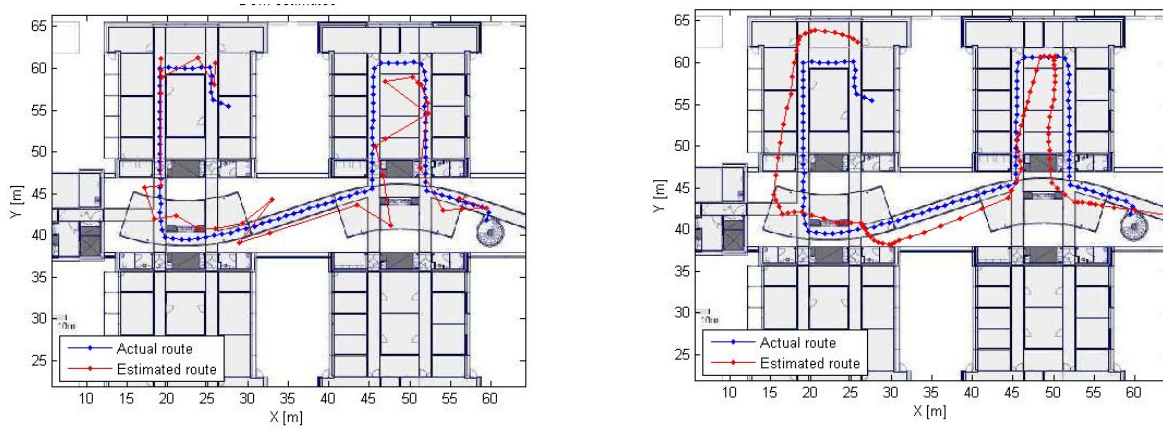


Figure 22. 2nd floor part of the route positioned with DCM (left) and DCM + EKF (right).

3.1.5 Sensor navigation results

The ZUPT algorithm developed in ILPO project was evaluated with MicroStrain sensor. The ZUPT based pedestrian tracking introduced in 2.3.2 was tested in Digitalo by walking the same route that was used to evaluate WLAN location fingerprinting. Without heading correction by electronic compass, the complementary EKF managed to predict correctly the length of the route segments and changes in the walking direction. The heading estimate started slowly to get inaccurate along the route as can be seen in Figure 23. Zero velocity updates were correctly detected during each stance phase and velocity estimate was reset to zero (see Figure 24).

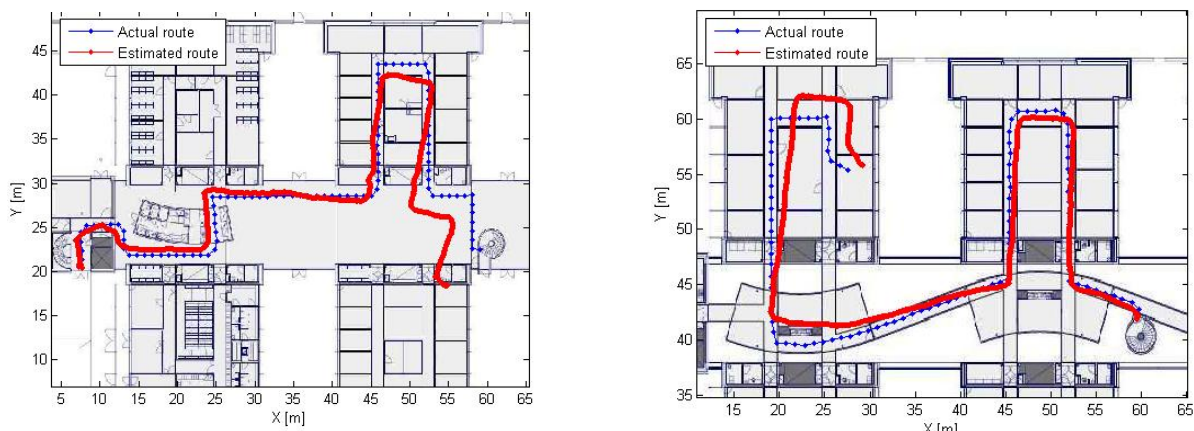


Figure 23. Digitalo route positioned with ZUPT based PDR (initial position and heading is given to the algorithm).

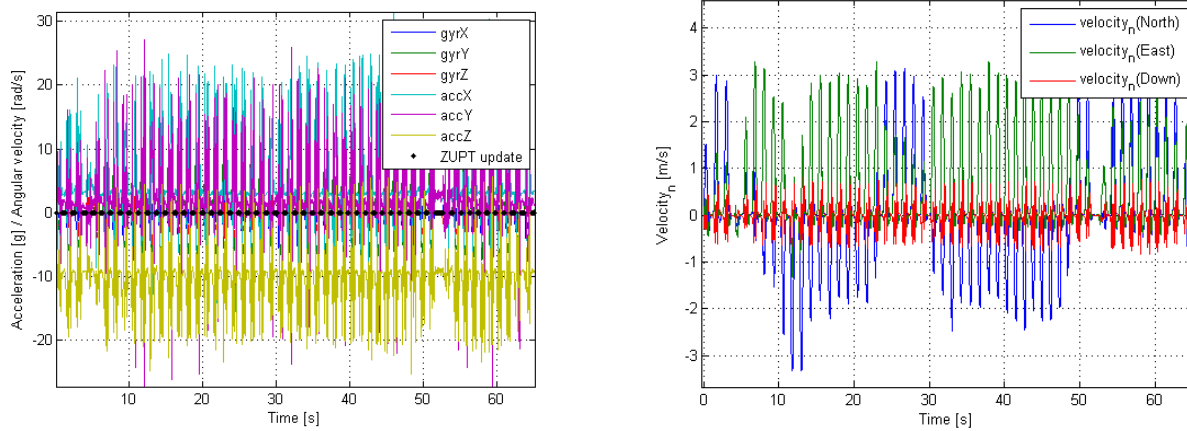


Figure 24. Detected Zero Velocity Updates (left) and corresponding velocity in navigation frame (right).

Floor change can also be detected with the implemented ZUPT based PDR. As a test, user walks the stairs up from 1st floor to 2nd floor. This measurement was compared to another measurement where the user had climbed up from 1st floor to 3rd floor. As can be clearly seen in Figure 25, the distinction between these two measurements is clear. Even the number of stairs can be calculated based on the Z-coordinate change.

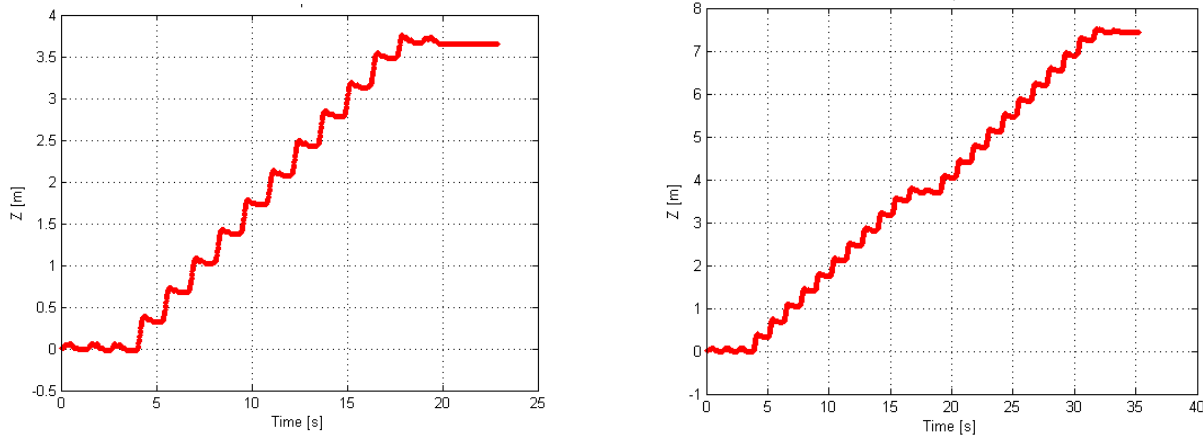


Figure 25. Walking upstairs from 1st floor to 3rd floor (left) and from 1st floor to 3rd floor (right).

Heading updates based on electronic compass were also introduced in the implementation of the complementary EKF – yet without complete success. Initial outdoor experiments on a baseball field indicated that the magnetometer based heading correction would indeed reduce the heading error caused by gyroscope drift and tilt errors. Indoors, the same effect was not achieved. One reason for this is the fact that soft and hard iron field distortions are far more prevalent inside buildings. Also the implemented filter may not be yet optimally tuned in order to tolerate noisy compass heading measurements and erroneous initial heading estimate (see Figure 26).

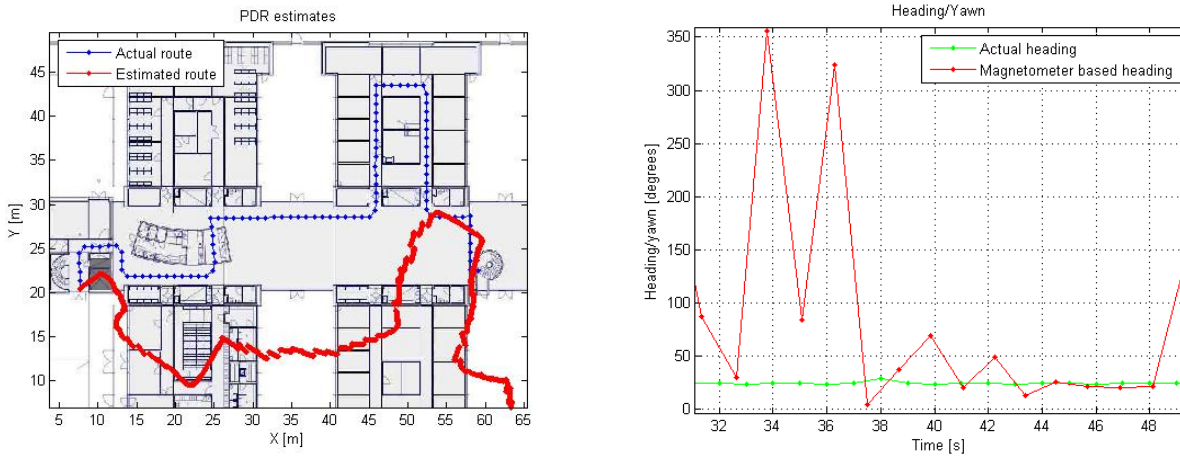


Figure 26. Error in the initial heading estimate and in heading updates yield poor route estimation (left). Actual heading and compass based heading along straight segment of the route near cafeteria (right).

3.1.6 Combining WLAN location fingerprinting and sensor navigation

As indicated earlier, the current implementation of the complementary EKF manages to estimate the travelled distance and changes in the walking direction even without proper heading updates provided by electronic compass. However, the filter does not provide complete autonomous positioning, because the initial position and heading needs to be known. Moreover, the gyroscope drift and tilt errors will result increasing error in the heading. In order to track the user without inputting the initial location and heading, the complementary EKF was combined with WLAN location fingerprinting (DCM) estimates and information about the floor plan using Particle Filter introduced in section 2.4. Floor plan images were converted into monochrome bitmaps and processed so that they indicate invalid user locations with black colour and valid areas with white. Processing included some manual adjustment, because e.g. door locations were not marked in the original floor plan image.

Preliminary results indicate good positioning accuracy especially if the route contains narrow hallways or corridors. In those places the confidence of the user location increases because the Map Filtering successfully limits the possible area where the user may reside. This is clearly seen in Figure 27. Particles first spread out when they enter the open area. After the sensor indicates straight movement to leftwards, the probability distribution gets smaller and particles residing lower part of the area will evidently be terminated. The implemented Particle Filter estimates the route in both floors quite successfully. Only in at the beginning of the measurements and in the large open hall the accuracy is noticeably degraded because of dispersing particle locations and poor DCM estimates. Results are shown in Figure 28.

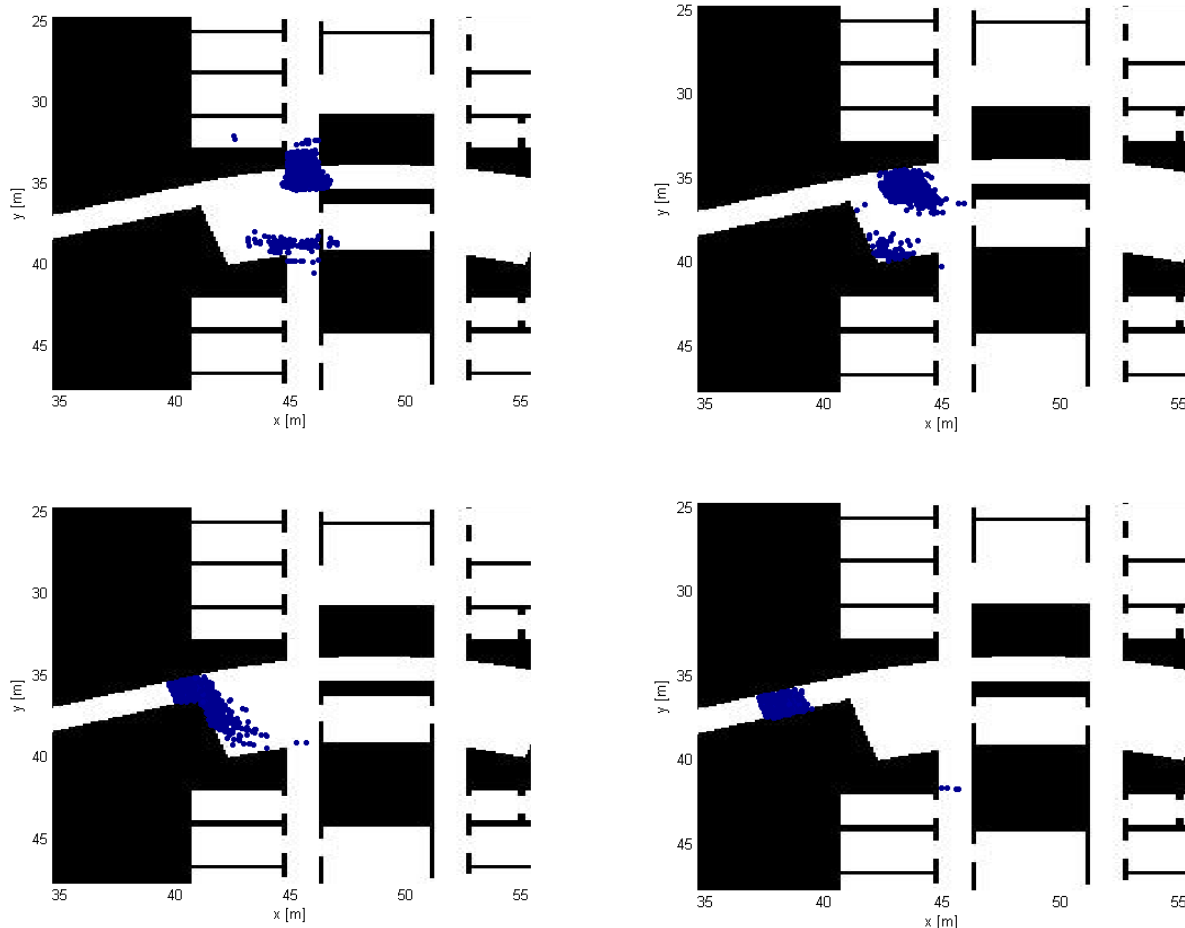


Figure 27. Four steps of Particle Filter indicating the probability distribution of the user along route in the 2nd floor of Digitalo.

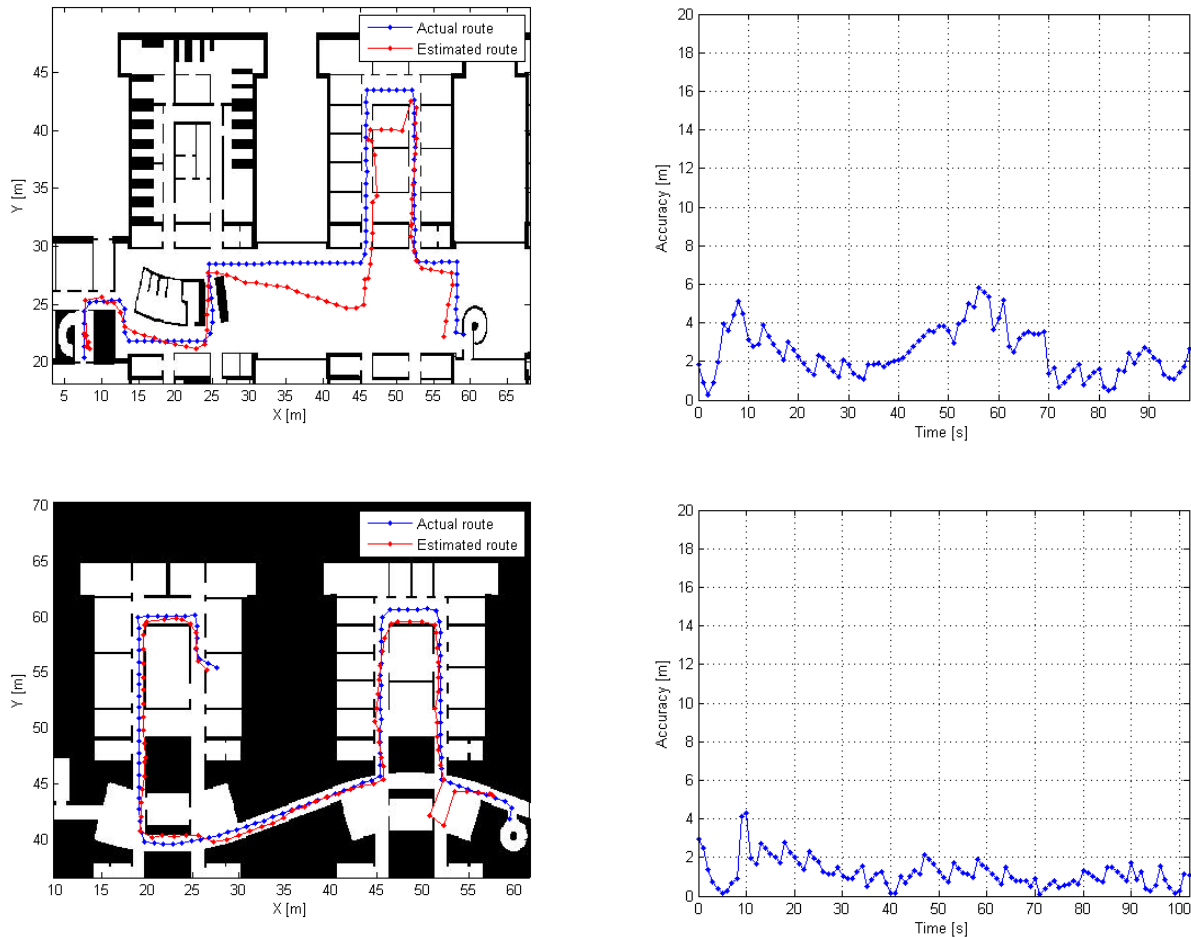


Figure 28. Particle Filter results from the route in Digitalo.

3.2 Preliminary trial in an underground facility

After the first tests in Digitalo, the positioning equipment was moved to an underground facility. The pre-trial there was seen as a rehearsal for the main pilot. For example, the new cables made for the pseudolite positioning system (for the paper mill pilot) were tested. Installing and uninstalling the system was practiced so that the time needed for Kvarnsveden pilot could be predicted. Part of the measurements was done in co-operation with VTT's own HYPEL project.

3.2.1 Trial area

The underground facility in bedrock contains two intersecting streets surrounded by large rooms. Metallic pipes and cable ladders are attached on the ceilings and walls. During the trial, there were usually a few cars parked in the hall. In addition, trailers, forklifts and research equipment like metallic tanks were in the area. The main trial area was about 820 m² of which 440 m² was covered with pseudolites.



Figure 29. Pictures from the underground facility. The end of the main street (above and down left) and the lobby with a door to staircase (down right).

3.2.2 Trial setup

For the trial, nine Linksys WRT54GL WLAN access points were placed around the underground facility for covering the trial area with the existing Cisco's access point. Antennas were removed from one AP (near the ramp for vehicles) in order to get smaller cell size.

In this trial, the same SSF's pseudolite positioning system as in Digitalo was used. The pseudolite network was constructed again with six pseudolites (see Figure 30). Two of the signal generators were replaced with new ones during the trial. The same antennas as in Digitalo trial were also used except for the last day the setup was changed to use two large helix antennas. The cabling was done using CAT7 cables specially made for the pseudolite positioning system in NOSE project. The pseudolites were attached on the metallic structures around the trial area. Two of the pseudolites were set at 4.40 meters and the other pseudolites at 6.20-6.60 meters. In planning the setup, special attention was paid to the pseudolite positions and antenna directions to ensure as pure LOS as possible in the main measurement area. The reference antenna was placed above the measurement area at 3.76 meters in order to ensure that nothing would block the signals between the reference antenna and the pseudolites during the trial.

In the underground trial, the local coordinate system was more difficult to create as in Digitalo. The hall is an underground place where only a few straight surfaces can be utilized in measuring. The coordinates of the pseudolites and the reference antenna were measured using a plumb line, a measuring tape and a laser distance-meter as accurate as possible.



Figure 30. The trial area and part of the setup. Pseudolite antennas (red symbols) and WLAN access points (blue symbols) with pseudolite (dark red hatched) and WLAN (light blue hatched) trial areas.

In the following, some pictures from the underground setup are shown.



Figure 31. The Sarantel helix antennas of the pseudolites number 1 (left) and 2 (right).



Figure 32. The large helix antenna (left) and the signal generator (right) of the pseudolite number 4.

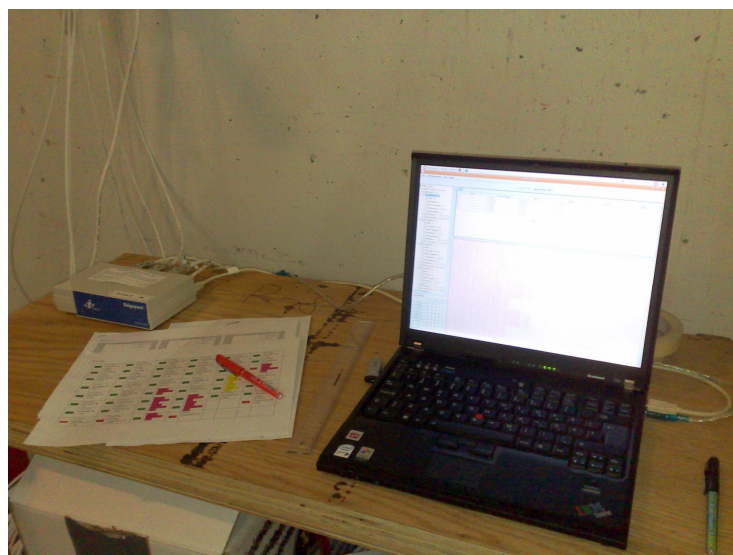


Figure 33. Master control station (MCS).

3.2.3 Pseudolite measurement results

Like in Digitalo trial, the operating range of the pseudolite configuration was checked first. 37 reference points (see Figure 34) were used to collect static measurement data.



Figure 34. Reference points used to collect position estimates. Green colour shows the best operating range of the pseudolite position system using continuous signals, yellow a bit problematic areas and red the areas where reliable position estimates couldn't be reached.

The measurement unit was manually initialized at RP23. After that, the receiver was moved to RP24, RP25, RP26 and RP27 in this order and about 60 position estimates were collected for every RP. The receiver was then initialized again and the rest of the reference points at the same row, RP 22 and RP 21, were measured. If the border of the operating range was reached at some point, the measurement unit was manually initialized again at RP23 in order to proceed with the remaining RPs. The sampling rate was 1Hz and all the pseudolites were synchronized in continuous signal mode.

Table 5. Results from the reference point measurement using continuous signals.

RP81	3-4 PLs Rel. fix 0.8m	RP11	4-5 PLs Rel. fix 0.1m	RP21	5 PLs Rel. fix 0.4m	RP31	5-6 PLs Rel. fix 1.1m	RP41	4-6 PLs Rel. fix 1.5m	RP51	4-5 PLs Mostly rel. fix 1.5m
RP82	4-6 PLs Rel. fix 0.2m	RP12	4-6 PLs Rel. fix 0.3m	RP22	4-5 PLs Rel. fix 0.2m	RP32	4-6 PLs Rel. fix 1.2m	RP42	4-6 PLs Rel. fix 1.3m	RP52	3-6 PLs Mostly rel. fix 1.9m
RP83	4-6 PLs Rel. fix 0.7m	RP13	5-6 PLs Rel. fix 0.8m	RP23	5-6 PLs Rel. fix 0.1m	RP33	5-6 PLs Rel. fix 0.3m	RP43	4-6 PLs Rel. fix 1m	RP53	4-6 PLs Rel. fix 1.6m
RP84	6 PLs Rel. fix 1m	RP14	4-6 PLs Rel. fix 0.6m	RP24	5-6 PLs Rel. fix 0.15m	RP34	6 PLs Rel. fix 0.5m				
RP85	4-6 PLs Rel. fix	RP15	4-6 PLs Rel. fix	RP25	4-5 PLs Rel. fix	RP35	4-6 PLs Rel. fix	RP61	3-5 PLs Rel. fix	RP71	4-5 PLs Rel. fix

	0.7m		0.4m		2.6m		1.5m		1.5m		2.0m
RP86	4-6 PLs Rel. fix 1m	RP16	4-6 PLs Rel. fix 1.3m	RP26	5-6 PLs Rel. fix 2.7m	RP36	4-6 PLs Rel. fix 3.9m	RP62	4-5 PLs Rel. fix 0.4m	RP72	3-5 PLs Rel. fix 2.3m
RP87	4-6 PLs Rel. fix 1.2m	RP17	3-6 PLs Rel. fix 1.6m	RP27	3-6 PLs Rel. fix 4.5m	RP37	3-6 PLs Mostly unrel. fix 2.6m	RP63	3-4 PLs Mostly unrel. fix 3.9m	RP73	4-5 PLs Rel. fix 1.6m
RP88	3-6 PLs Mostly unrel. fix 1.4m	RP18	3-6 PLs Mostly unrel. fix 2.6m	RP28	3-6 PLs Rel. fix 7.3m	RP38	3 PLs Unrel. fix PRN64,65			RP74	3-5 PLs Unrel. fix PRN60,64

Position estimates were also collected statically in some reference points using pulsed signals with four pseudolites. The reference points included those that had high positioning error in the continuous signal case, i.e. points 25-27 and 35-37, in order to test whether the pulse signal mode improves the system performance. The results are shown in the following table.

Table 6. Results from the reference point measurement using pulsed signals.

RP21	4-6 PLs Reliable fix 1.4m	RP31	5-6 PLs Reliable fix 0.8m
RP22	4-6 PLs Reliable fix 0.6m	RP32	5-6 PLs Reliable fix 0.7m
RP23	5-6 PLs Reliable fix 0.2m	RP33	6 PLs Reliable fix 0.9m
RP24	6 PLs Reliable fix 0.5m	RP34	5-6 PLs Reliable fix 1.6m
RP25	5-6 PLs Reliable fix 0.8m	RP35	4-6 PLs Reliable fix 1.5m
RP26	5-6 PLs Reliable fix 0.9m	RP36	5-6 PLs Reliable fix 1.1m
RP27	5-6 PLs Reliable fix 0.8m	RP37	4-6 PLs Reliable fix 0.8m

Using continuous signals, the coverage area included almost all the reference points as expected. The biggest errors appeared near pseudolites and in the areas where the corner blocked direct signals from some pseudolites. Using pulsed signals improved the results in problematic areas. Generally, the position estimates had small variance and the accuracy provided was much better compared to the results from Digitalo trial.

Position estimates were also collected by moving with fixed velocity along different routes. In the measurements either continuous signals or pulsed signals (RTCM) were used. The system was synchronized so that SNRs for the pseudolites were with the continuous signals in the ranges of 39 (PRN60), 41-43 (PRN63) and 44-46 (PRN64-65) and with the pulsed signals in the ranges of 40-43 (all). About half of the measurements were made by initializing the measurement unit at a certain reference point and the rest of the measurements were made without manual initialization to see how the system would perform in more realistic situation.

Again, different routes inside the “coverage area” were recorded and each route was sampled two or three times (Route a, b and c). One route, which was also measured with WLAN location fingerprinting, ended outside the best positioning area.

When measuring without manual initialization the measurement GPS receiver was started and moved around the best positioning area as long as it took to get a fix. The system generated the first position estimate usually in 30 seconds. After that the measurement unit was moved to the starting point of the route and the recording of the measurement was started. From time to time the receiver had to be restarted before the fix was found.

An annoying feature of receiver hardware was detected when making the measurements with higher speeds. The hardware couldn't process position estimates with the sampling rate used (1Hz). As it was seen important that the measurer could see the progress in action, the measurements were decided to continue with slower speeds. According to SSF, the problem can be solved later by passing the hardware and taking the raw data directly to the computer.

The results show that the system performed a lot better than in Digitalo case. When measuring with manual initialization, tracking was usually pretty good and turns were detected well. The same kind of constant bias as in Digitalo wasn't detected. However, more detailed examination to the pseudolite signals (made by SSF) revealed that in some parts of the area the carrier phase of some signals changed incorrectly.

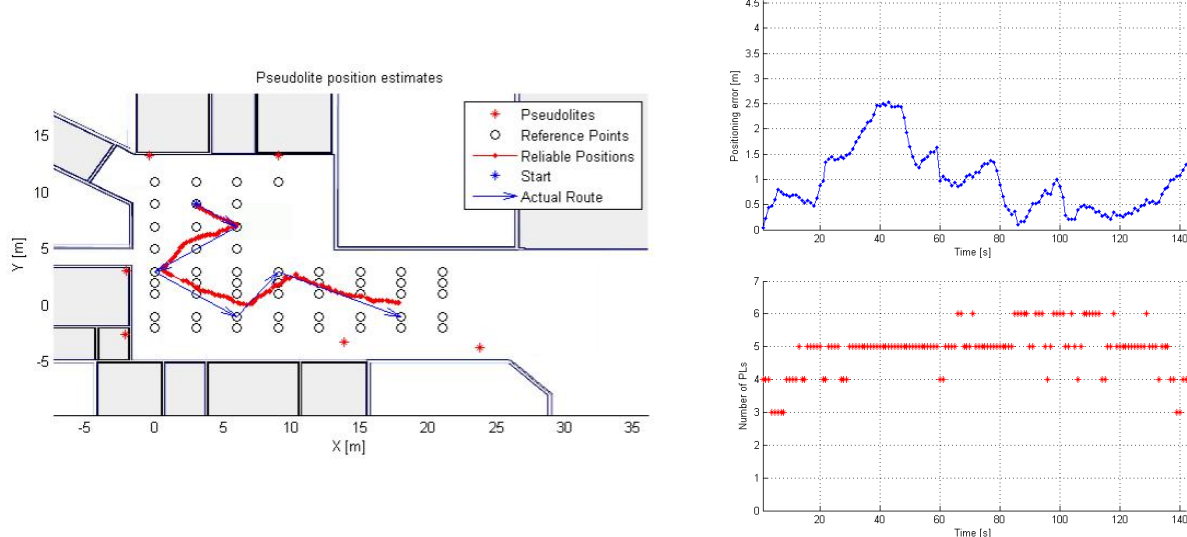


Figure 35. Route 2B_6b.

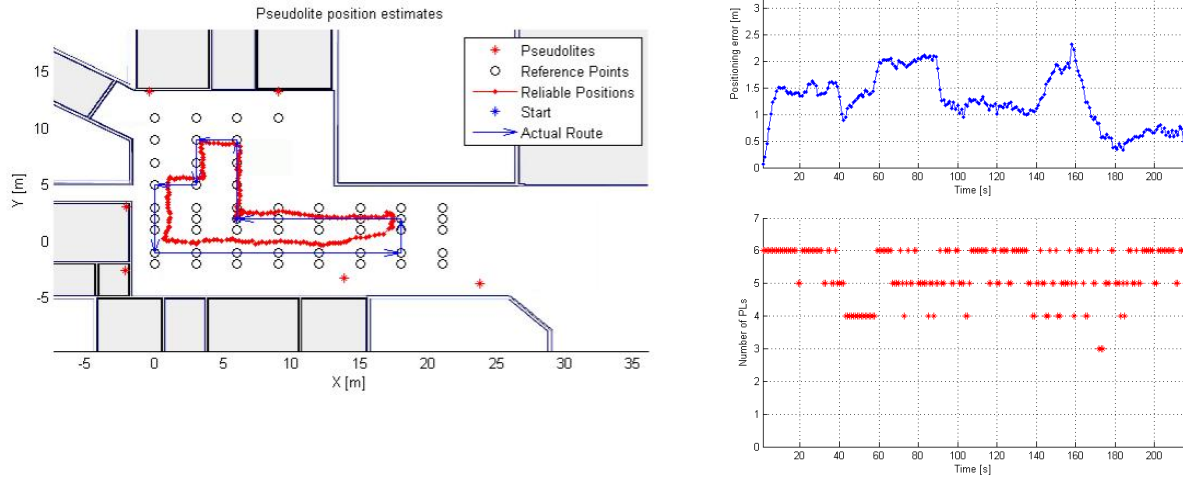


Figure 36. Route T4_5c.

The navigation algorithm generated quite big jumps to the position estimates. The following example shows two typical cases. Occasionally the jump was done to the wrong direction and sometimes to the right direction to provide a lot better position estimate. In this example case, the accuracy in the ending part of the route was good because with the second jump the system eventually corrected the error in the initial position estimate.

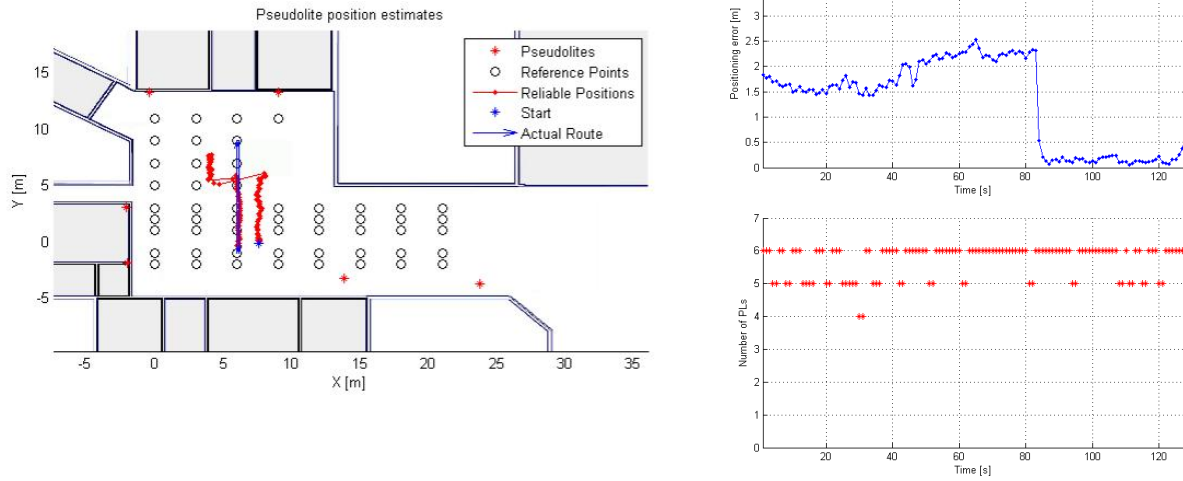


Figure 37. Route T6_13b.

During the pre-trial, the pseudolite configuration was changed twice. After the first measurements, pseudolite number 3 antenna was moved a bit to improve the better signal quality. In addition, the navigation algorithm was changed by SSF. The changes improved the accuracy, yet the system was still sensitive to cycle slips. In closed direct routes going back and forth on X or Y axis tracking was good and the estimated ending point was usually pretty close to the actual ending point. If the route was measured without manual initialization, the position estimates suffered from the constant error in initial position estimate. In the following figures, typical examples of measurements made in closed direct routes are presented. The first route was measured with manual initialization and the second in free mode.

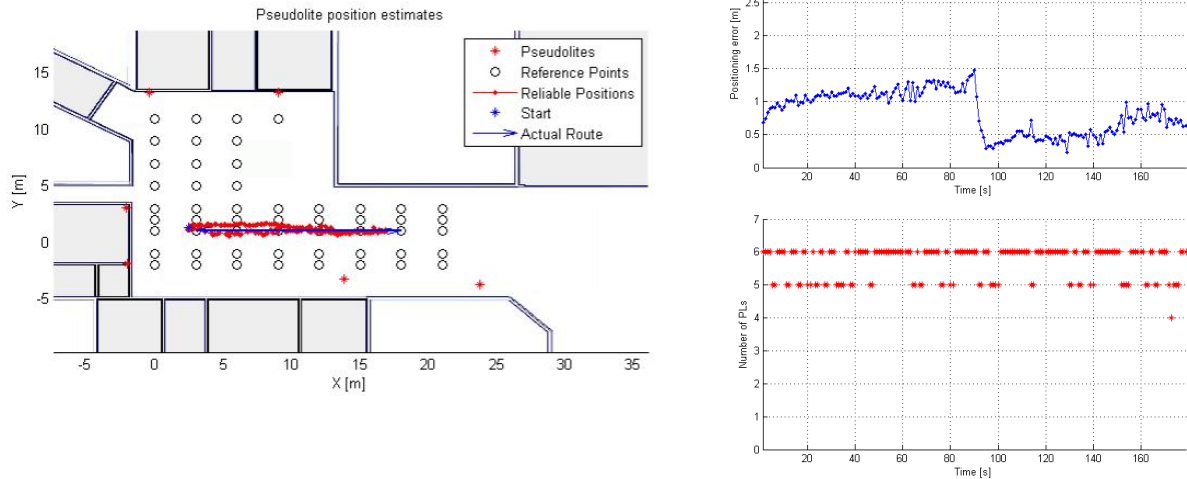


Figure 38. Route T7_1a measured without manual initialization.

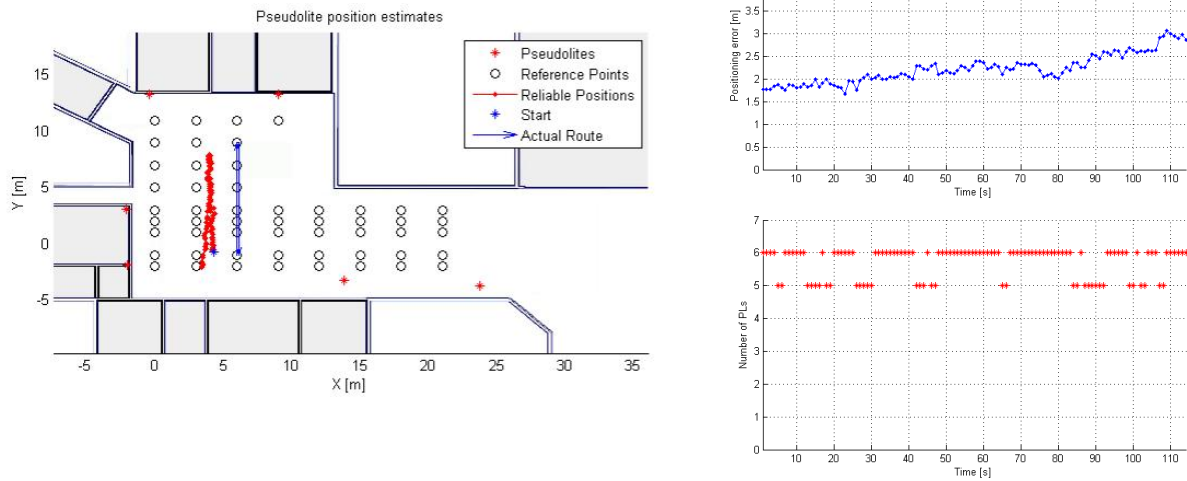


Figure 39. Route T7_13a measured without manual initialization.

The second change to the configuration was done to find out what kind of effects usage of different kind of antenna would cause to the results. The small helix antenna of pseudolite number 2 was replaced with a large helix antenna. In the following examples, first two measurements were made before changing the configuration and the next two measurements after it. Two of the measurements were made with manual initialization and the other two measurements in free mode. In all measurements, the system was synchronized using pulsed signals.

As it can be noticed on the following figures, the narrower antenna pattern improved the results further on the main street near the rightmost border of the pseudolite measurement area. Behaviour in closed direct routes was also a bit better than before although fixes were harder to get in the upper part of the measurement area. The result was quite expected because changing a pseudolite antenna affects its coverage area. The sensitivity to cycle slips wasn't improved.

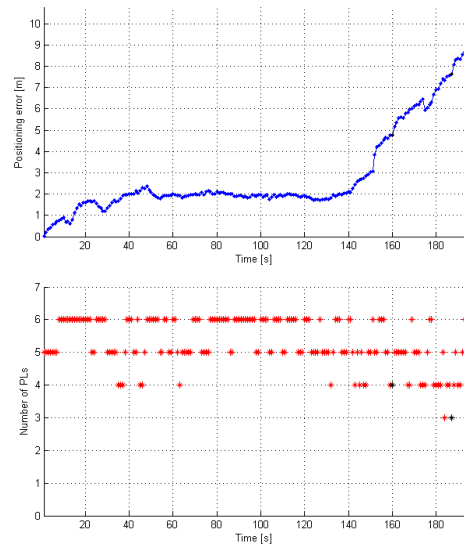
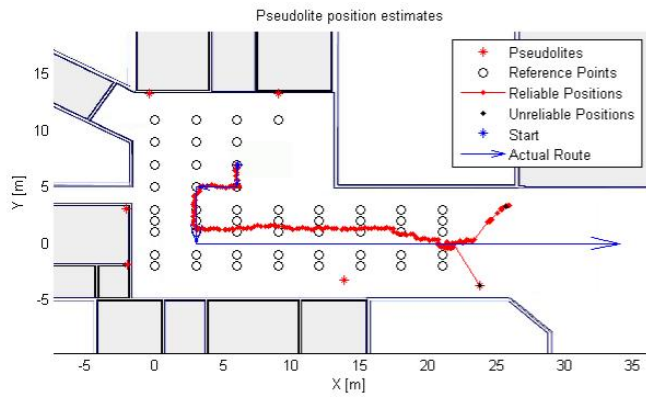


Figure 40. Route T7_19a1 measured with manual initialization.

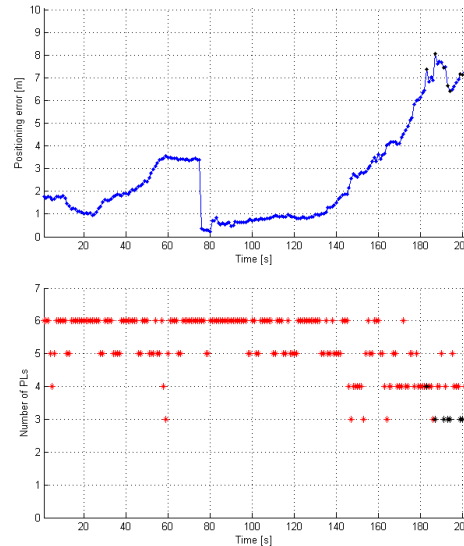
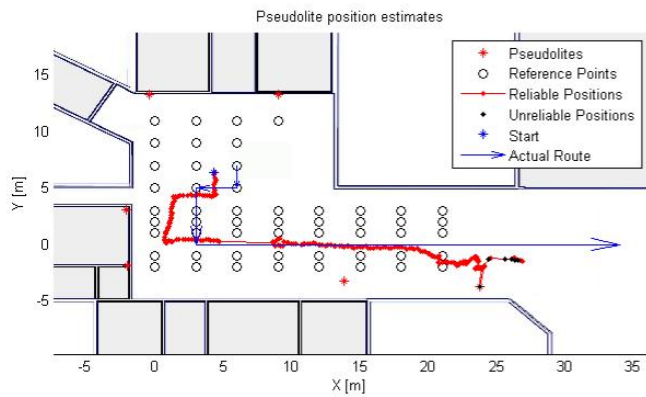


Figure 41. Route T7_19a2 measured without manual initialization.

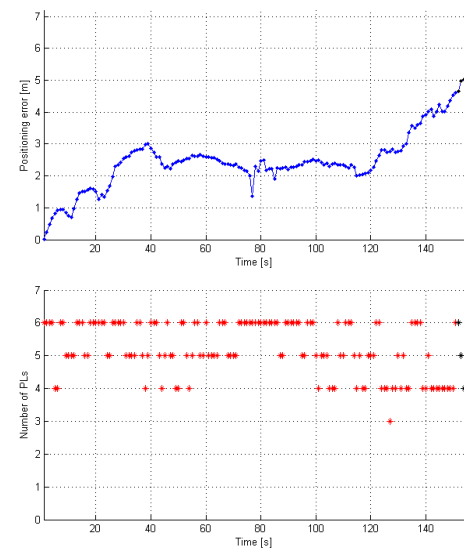
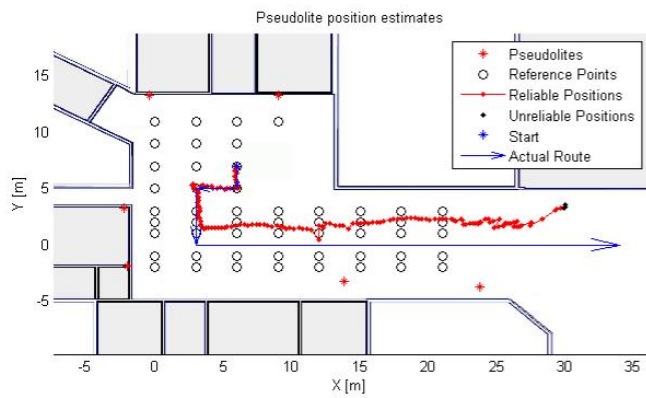


Figure 42. Route T8_19a1 measured with manual initialization after configuration change.

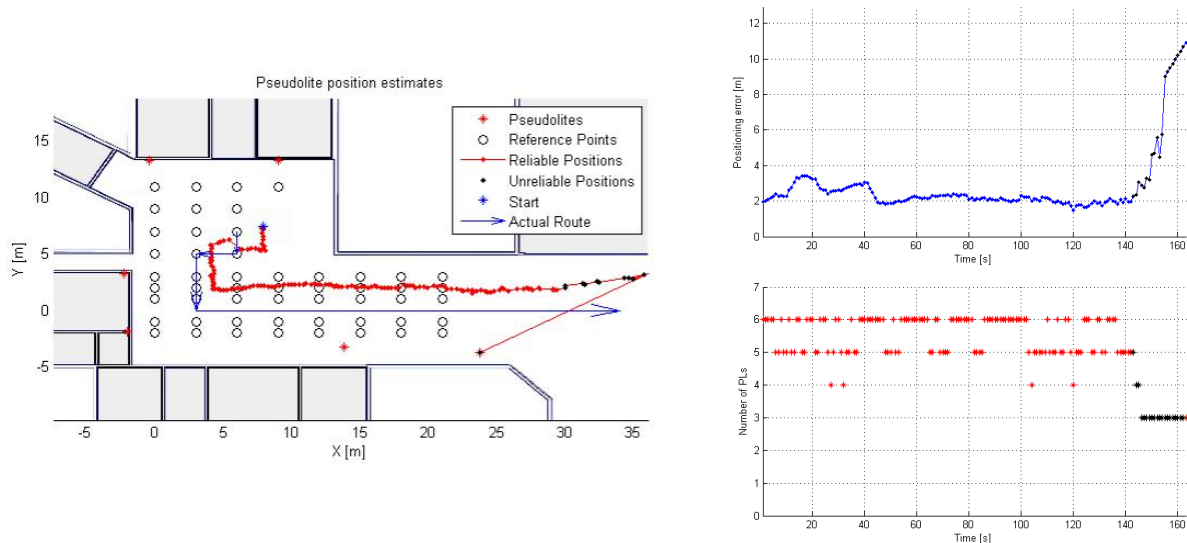


Figure 43. Route T8_19a2 measured without manual initialization after configuration change.

The positioning errors from the selected routes are presented in the following table. Some test results are also reported in Laitinen and Ström's publication [19].

Table 7. Positioning errors of selected routes in the underground trial.

Route	Mean positioning error [m]	Standard deviation
Route T2B_6b	0.96	0.64
Route T4_5c	1.27	0.50
Route T6_13b	1.29	0.87
Route T7_1b	0.84	0.32
Route T7_13a	2.22	0.32
Route T7_19a_1 ⁴	2.05	0.94
Route T7_19a_2 ⁴	1.83	1.13
Route T8_19a_1 ⁴	2.17	0.60
Route T8_19a_2 ⁴	2.27	0.41

During the trial, some interference was caused by a fork-lift and a crane. When a fork-lift drove to the measurement area close to pseudolite number 3 a 4 cm error in the synchronization state of the pseudolite was noticed immediately. When the fork-lift drove back and forth, the error increased to 3.8 meters. After the pseudolite number 3 was moved to a new position, the feature disappeared. Furthermore, the crane caused losing the synchronization once which could be a problem in the Kvarnsveden pilot.

As a conclusion, the underground hall was more suitable for pseudolite positioning than Digitalo. The space in the hall allowed building up a better pseudolite setup. Pseudolites were possible to attach higher above the measurement area so the near-far problem didn't cause as much limitations to the usage of the area as in Digitalo. In the traffic hall, there were also more possible places to attach the antennas. However, indoor environment is always problematic and unforeseeable. Even though the setup was built as well as possible (using the

⁴ Route 19 ended outside the pseudolite positioning area. 85% of position estimates (from the beginning of the route) was used to calculate the positioning error.

available equipment) some changes to the configuration were necessary to improve the performance of the system. Further investigation is still needed to find out the reasons for distortion of the signals so that this kind of behaviour could be predicted and prevented in the future. If possible, more tests with different kind of antenna configurations should also be made.

3.2.4 WLAN location fingerprinting results

Similarly to Digitalo measurements, the accuracy of DCM and DCM + EKF was evaluated by collecting first reference fingerprints (80) from the area where the positioning was carried out. Reference fingerprints were again collected with Fujitsu-Siemens Pocket Loox and Site Survey tool. The test route started from the storage area where the pseudolite system was installed. The route passes through the main pathway to the lobby nearby the elevators and emergency staircase. Total length of the route was around 100m. The route was repeated 3 times. Numerical results are shown in Table 8.

Table 8. DCM and DCM+EKF results from the measurements carried out in the underground facility.

Route:	Samples:	Mean [m]:	CEP 50% [m]:	CEP 67% [m]:	CEP 95% [m]:	Max error [m]:
RH11, DCM	104	4.2	3.9	4.9	8.3	11.0
RH12, DCM	104	3.8	3.3	4.8	8.0	11.9
RH13, DCM	104	4.3	4.1	5.1	9.5	12.7
RH11, DCM + EKF	104	4.2	3.3	4.9	8.8	10.8
RH12, DCM + EKF	104	3.6	3.5	4.5	7.8	9.8
RH13, DCM + EKF	104	4.3	4.3	5.2	9.0	12.0

The average accuracy using DCM is around 4m and maximum error is over 10m. Again the low scanning rate of the laptop used in the test routes might be one of the reasons for the modest accuracy. On the other hand, almost the whole area is relatively open except the last part of the route near the elevators. This fact will definitely set limits to the accuracy level that can be achieved with WLAN location fingerprinting. Extended Kalman Filter improves the results slightly but the effect is quite small in terms of accuracy in meters. The difference can be more easily seen in Figure 44.

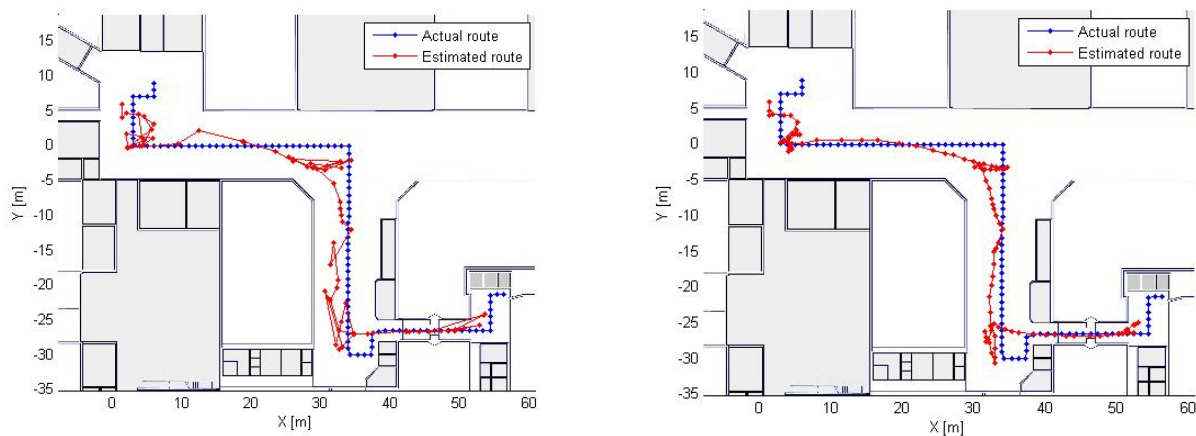


Figure 44. Underground route positioned with DCM (left) and DCM+EKF (right).

4 Kvarnsveden pilot 2008

The first positioning pilot was carried out in Kvarnsveden paper mill on 8.-12.9.2008.

4.1 Trial area

The area for pedestrian positioning trials was planned around the learning and the field operator route. The route circulated on two floors. It started from the ground floor, where there were two larger corridors on the route. Otherwise, it circulated in a labyrinthine jungle of huge tanks and pipes. The dominant materials on the route are metal and concrete which makes the environment quite hostile for radio wave propagation.



Figure 45. Pictures from the pilot area on the ground floor.

On the upper floor (operation floor), the route passed the head of the paper machine and went to the main corridor. This part of the route is mostly open space, but behind the paper machine the environment changes into a more enclosed one. Like on the ground floor, the main materials here are also metal and concrete. The main hall has large windows.



Figure 46. Pictures from the pilot area on the operation floor.

4.2 Trial setup

For the trial, 15 Linksys WRT54GL WLAN access points were placed around the ground and the operation floor in order to cover the trial area. Nine APs were set to the operation floor (see Figure 48) and the rest of the APs were distributed to the ground floor (see Figure 47). The access points were placed on the floor or on top of the electric board at 1.3 meters. One of the APs was on the landing.

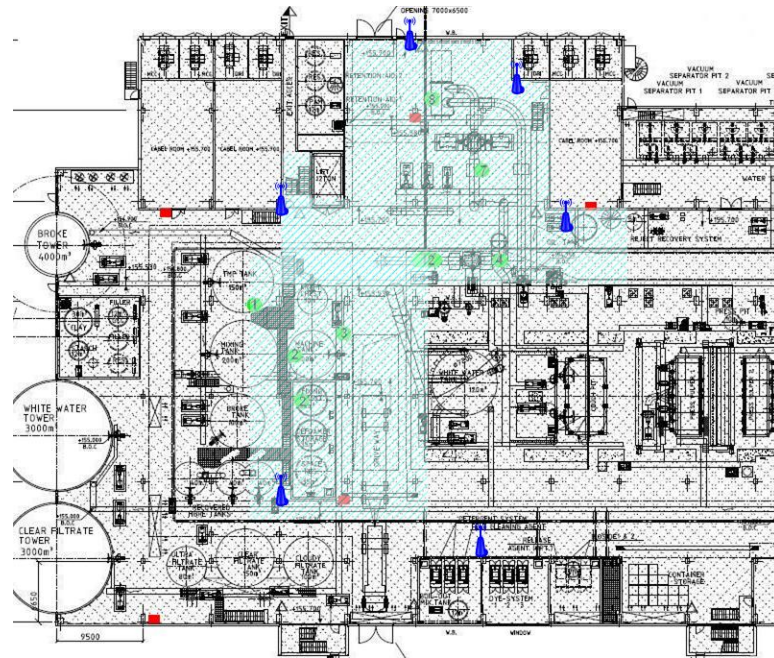


Figure 47. WLAN setup and trial area on the ground floor.

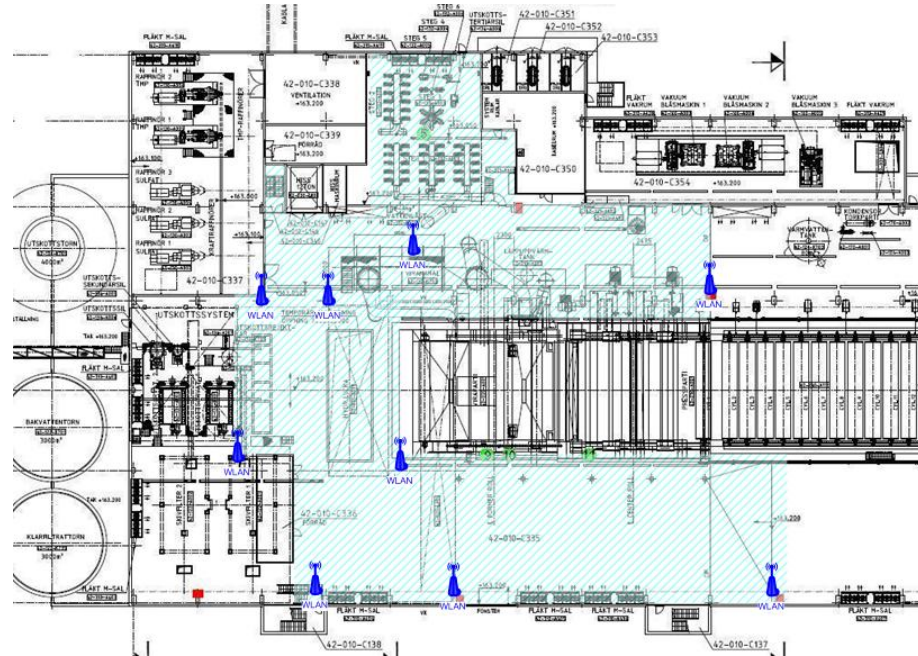


Figure 48. WLAN setup and trial area on the operation floor.

The pseudolite positioning system was built using Space Systems Finland's pseudolites and antennas. The following devices were used:

- Six pseudolites
- Five Sarantel helix antennas and one large helix antenna
- A laptop as a Master Control Station (MCS) running Linux Ubuntu (kernel 2.6.22-14) and SSF's server software
- Fastrax iTrax03EvaluationKit GPS receiver as a reference receiver running SSF's software
- Edgeport 8 port USBtoSerial adapter
- CAT7 cabling

Another Fastrax iTrax03EvaluationKit GPS receiver was used for navigation and positioning measurements. The firmware was modified by SSF.

The pseudolites were placed at the end of the main hall as depicted in the following Figure 49.

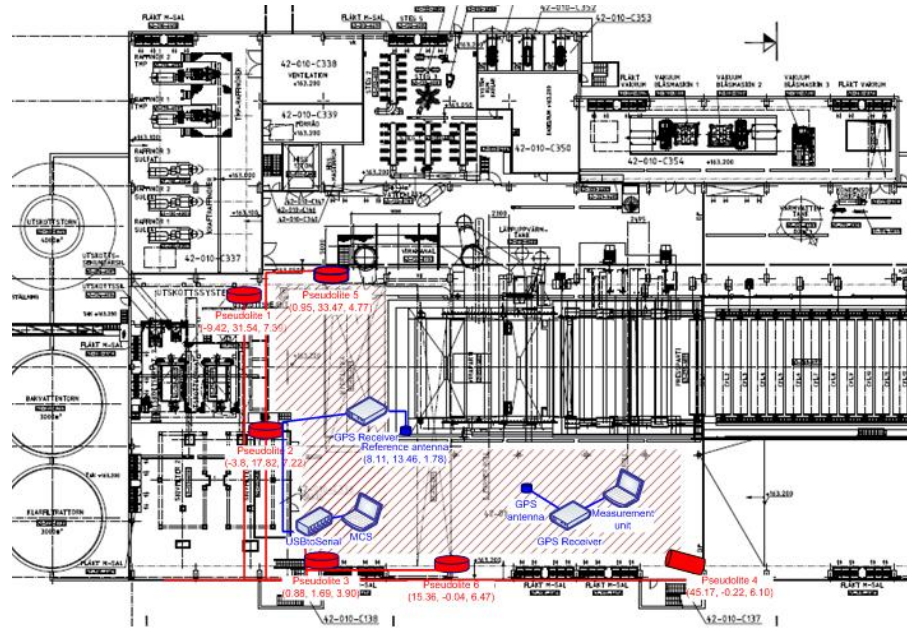


Figure 49. Pseudolite setup and trial area on the operation floor.

The pseudolite setup couldn't be built in Kvarnsveden as well as it was previously planned. The paper mill personnel could offer only an articulated jack for our use even if an articulated boom lift was asked. The planned antenna positions couldn't be reached with it, so the pseudolite antennas had to be placed at lower heights. The paper mill environment also caused limitations for the placing the cables.

Pseudolite antennas were attached on the railings and on the metallic structures on the walls. Each pseudolite was connected to the master control station via CAT7 cables and the USBtoSerial adapter. The reference receiver was connected directly to the MCS via a CAT7 cable. The antenna of the reference receiver was placed on the railing at the corner of the paper machine. For positioning, a local coordinate system and a grid for route measurements were created and marked on the floor. The coordinates of the pseudolites and the reference antenna as well as the route marks were measured using a plumb line, a measuring tape and a laser distance-meter. In planning the setup, special attention was paid to the pseudolite positions and antenna directions.

In the following, there are some pictures from the trial setup.



Figure 50. The small helix antennas of the pseudolites number 1 (left) and number 5 (right).

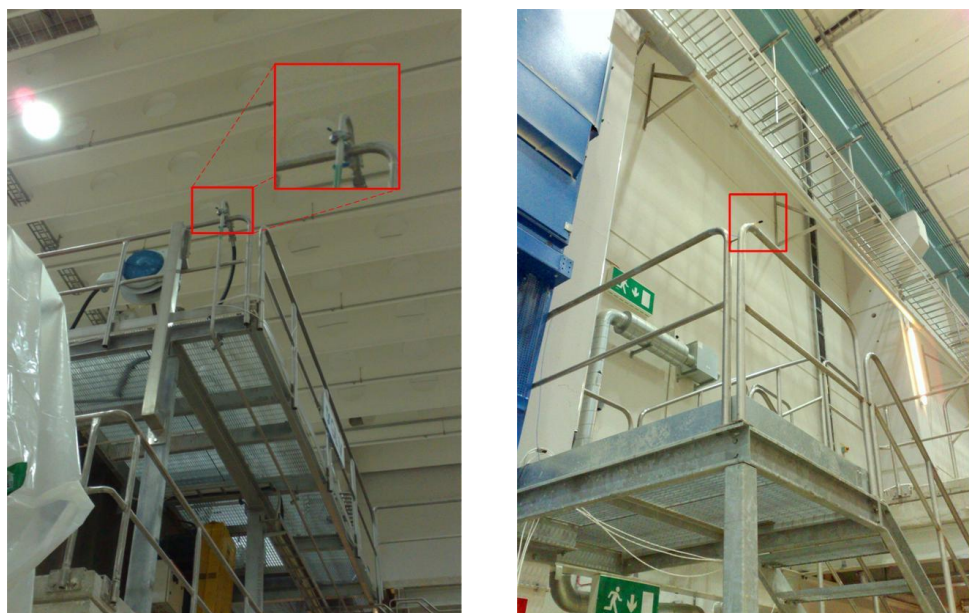


Figure 51. The small helix antennas of the pseudolites number 2 (left) and number 3 (right).



Figure 52. The signal generator of the pseudolite number 3 (left) and the large helix antenna of the pseudolite number 4 (right).

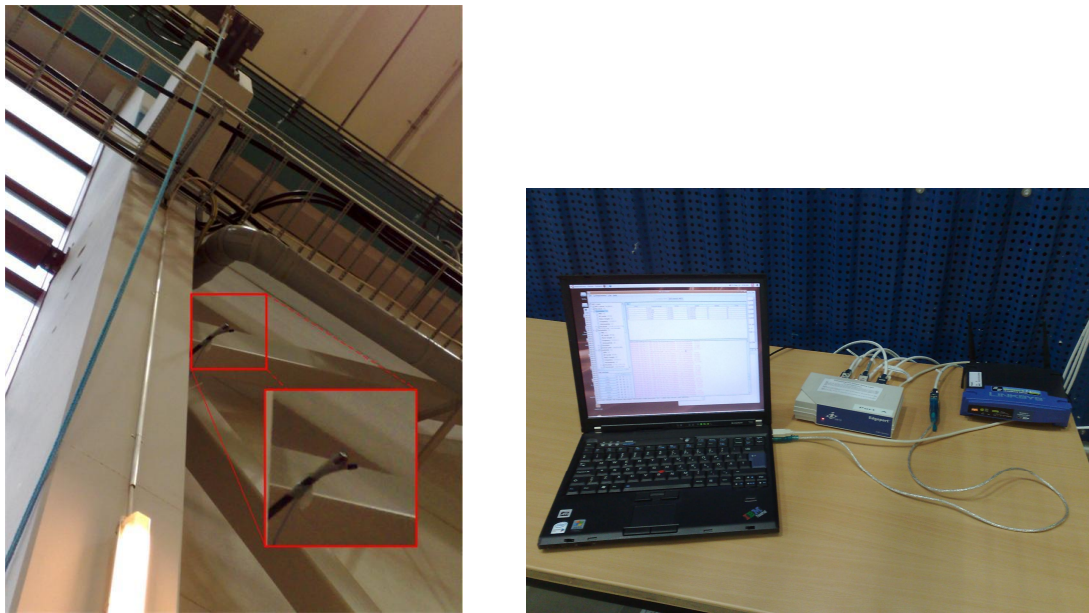


Figure 53. The small helix antenna of the pseudolite number 6 (left), MCS laptop, Edgeport USBtoSerial device and one of the WLAN access points (right).

An IMU (Microstrain 3DM-2GX), consisting of 3-axis gyros, accelerometers, and magnetometers, was attached tightly to the right shoe of the pedestrian as shown in Figure 10. See Annex 1 for details and specs of the sensor system.



Figure 54. IMU (Microstrain 3DM-2GX) attached to a shoe.

4.3 Pseudolite measurement results

The schedule (1 week) for the pilot was tight for pseudolite measurements. It was decided to pass the reference fingerprint measurements because they would have taken too much time. The coverage area could be estimated based on pre-trial results. For the trial area, one main route, which circulated in the pilot area, was planned. The main route was measured with all three positioning systems: WLAN location fingerprinting, pseudolites and sensors. In addition, 4-5 simple routes were planned for pseudolite measurements.

Building up the pseudolite system took 2.5 days. First the system was synchronized using continuous signals. The system was synchronized so that SNRs for the pseudolites were in the

ranges of 39-45 for all pseudolites and with the pulsed signals in the ranges of 40-43 (for all pseudolites). For saving time, more than half of the measurements were made by initializing the measurement unit at a certain starting point. The rest of the measurements were made without manual initialization in order to see how fast the system could find the first fixes and what kind of initial position estimates it could provide. Each route was usually sampled twice (Route a. and b.). In some problematic cases the measurement was done three times.

At first, a couple of routes were measured using continuous signals to get the first impression how the system would work in the paper mill environment. Results were promising (see Figure 55 and Figure 56). In closed direct routes going back and forth on X and Y axis, the position estimates reflected the length of the actual route. Tracking was quite good and positioning error was at the same level as in previous measurements in the underground trial. Nevertheless, the estimated route (see Figure 55) bent strongly towards the paper machine. In addition, relatively good first fixes were hard to get in a reasonable time.

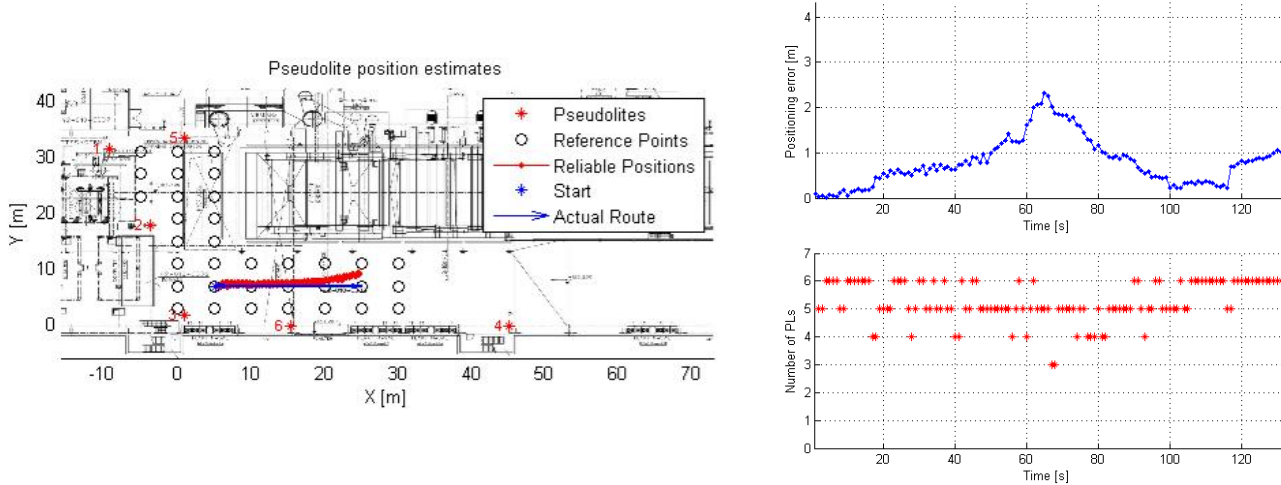


Figure 55. Route T1_1a with manual initialization.

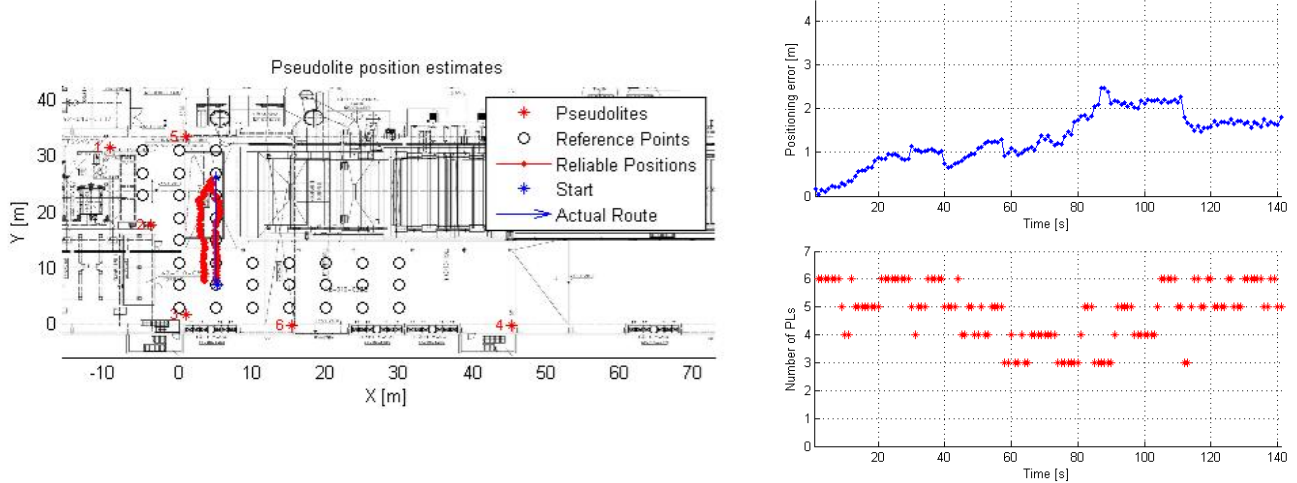


Figure 56. Route T1_2a with manual initialization.

After the first tests, pseudolites were changed to use pulsed signals. Results were partly unsatisfying. The system could get good enough fixes (closer than 1.5m) in a reasonable time for all four measurements made without manual initialization (see Figure 57). But, during the measurements, it was detected that the signals should be stronger. There was also a big

problem with the main route. The position estimate was unreliable close to the head of the paper mill in all three measurements.

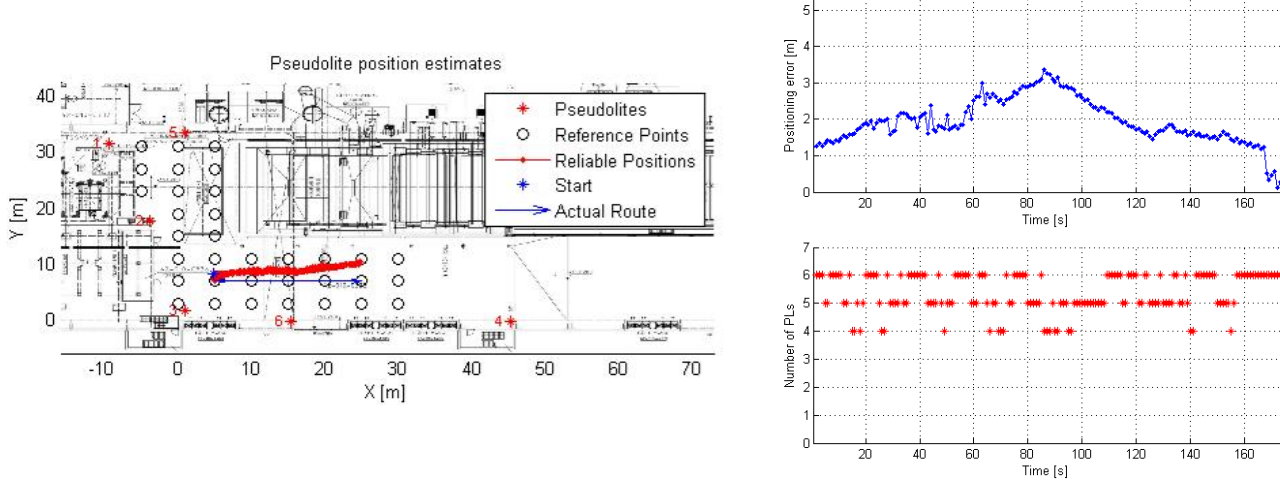


Figure 57. Route T2_1b without manual initialization.

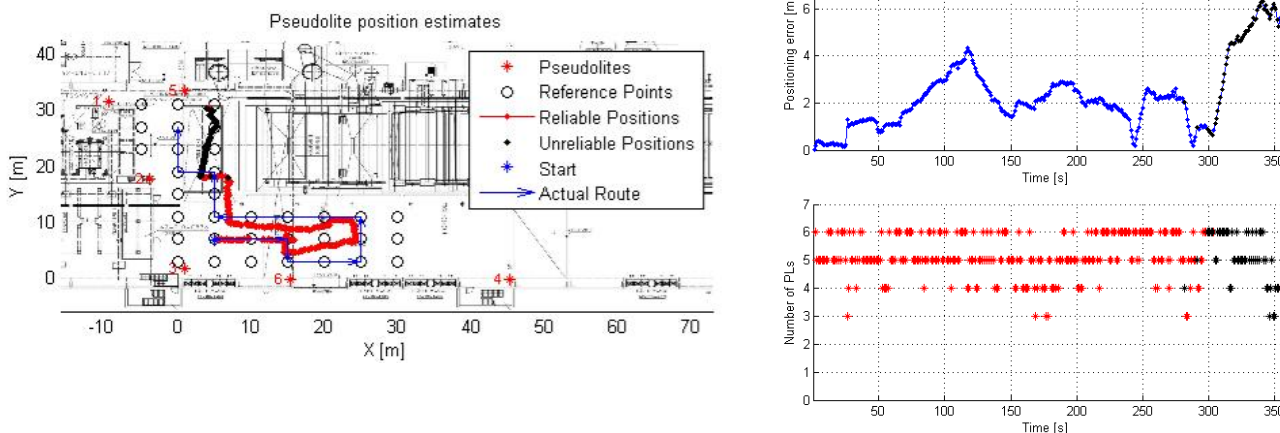


Figure 58. Route T2_4b with manual initialization.

Details in the synchronization had indicated problems with pseudolite number 1 and 2. For example, for those pseudolites attenuation had to be set much lower than for the rest of the pseudolites. The position of the pseudolite number 2 was also considered problematic (the LOS wasn't pure enough near the pseudolite) so the pseudolite was decided to be moved (see Figure 59). A better place for the pseudolite number 1 was hard to find so it was left in the old place. The antenna of the pseudolite number 3 was also slightly adjusted. It was turned to point more towards the main corridor. For the last day, the signal strengths of the pseudolites 2-6 were set higher.

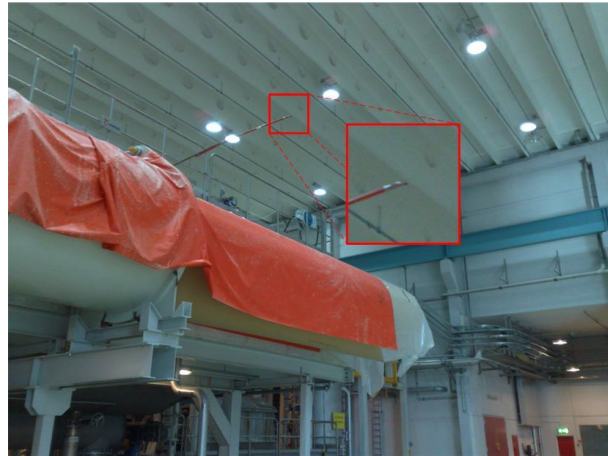


Figure 59. The new position of the pseudolite number 2 antenna.

The changes improved the synchronization of the pseudolite number 2 and the positioning results were better at the head of the paper machine (see Figure 60). The system was now able to provide reliable position estimates to the whole main route. Moreover, the first fix was easier to get. Usually the first position estimate was within 3 meters, but occasionally around 5 meter errors were detected. From time to time the system couldn't provide an initial position estimate in a reasonable time at all.

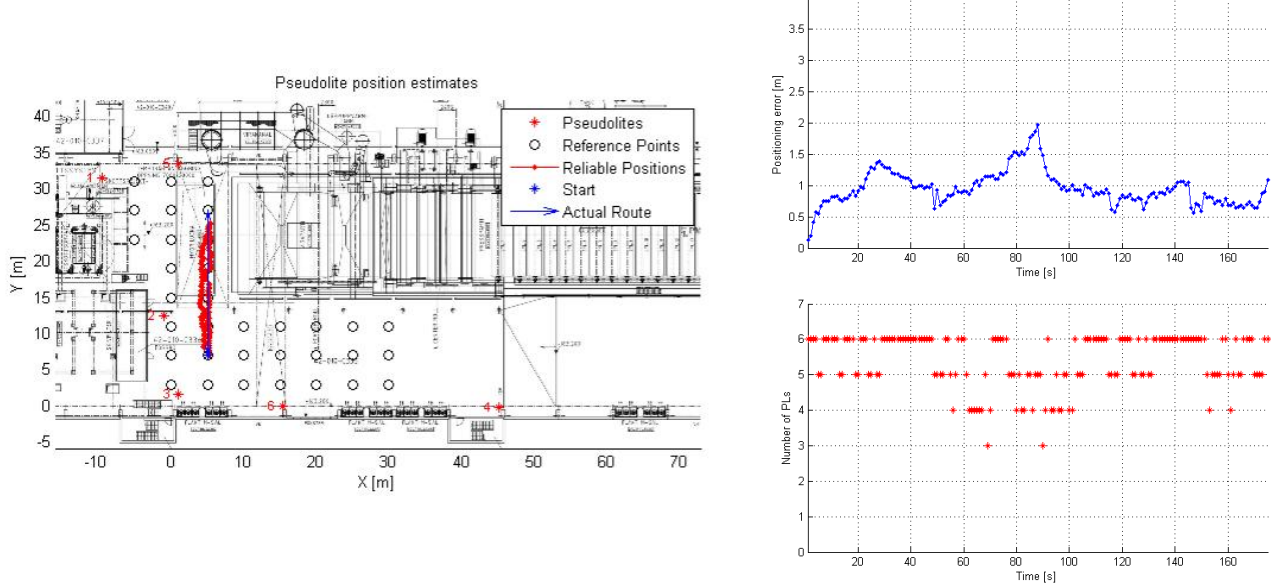


Figure 60. Route T4_2a with manual initialization.

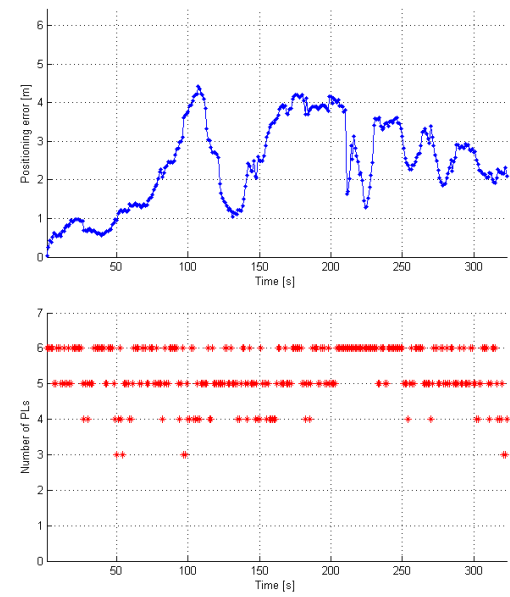
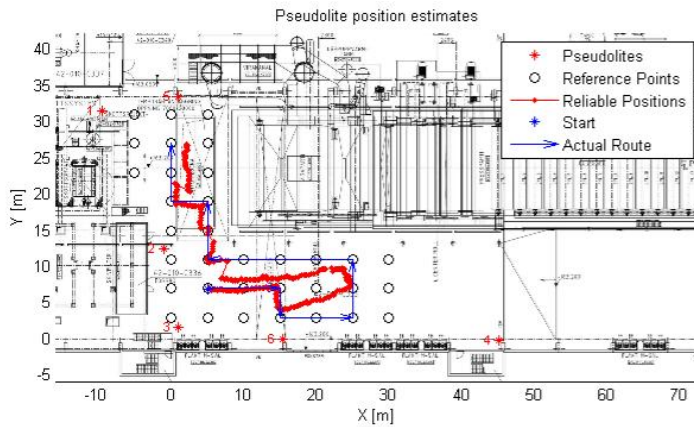


Figure 61. Route T4_4b with manual initialization.

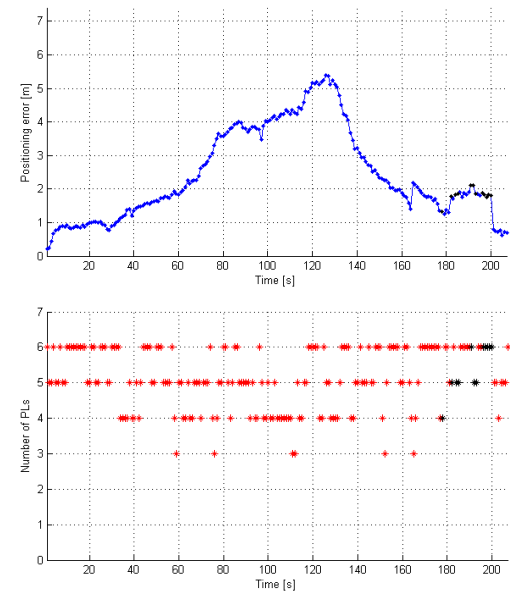
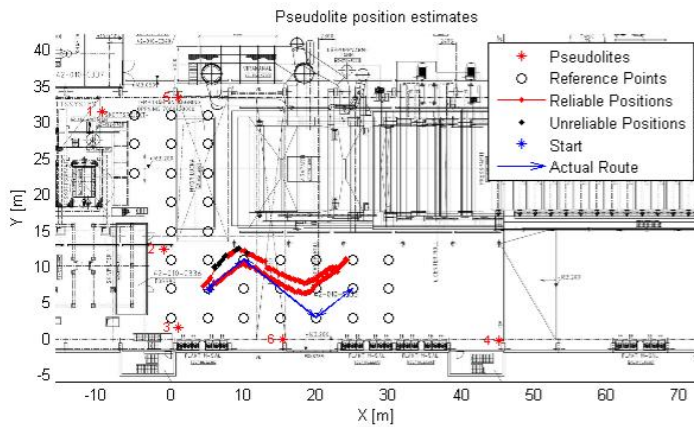


Figure 62. Route T4_6a_2 without manual initialization.

The positioning errors from the selected routes are presented in the following table.

Table 9. Positioning errors of selected routes in the paper mill pilot.

Route	Mean positioning error [m]	Standard deviation
RouteT1_1a	0.7891	0.5340
RouteT1_2a	1.3264	0.5955
RouteT2_1b	1.9547	0.6155
RouteT2_1c	1.1548	0.5548
RouteT2_4b	2.2789	1.4261
RouteT4_4a	2.2252	1.1072
RouteT4_4b	2.4149	1.1341
RouteT4_2a	0.9552	0.2814
RouteT4_6a_2	2.4390	1.3636

The environment in the paper mill trial was more challenging than in the underground trial. The metallic head of the paper machine, the closets on the wall and the railings all over were strongly reflecting. That can be seen from the results. Positioning errors and standard deviations were bigger than in the underground trial. The system was also more sensitive to cycle slips.

Even though, the pseudolite setup was tried to be made as well as possible, it is evident that the configuration wasn't as good as it could have been. The changes to the configuration improved the reliability. However, correcting the bending on the main corridor would have required such big changes to the pseudolite setup that wasn't possible during the pilot.

During the paper mill pilot, the system was working consistently. It stayed well synchronized. From the synchronization log, it was seen that there had been a short break in connection to the reference antenna which was repaired automatically. Any problems caused by passing fork lifts or cranes were not detected.

4.4 WLAN location fingerprinting results

Like in pre-trials, the accuracy of DCM and DCM + EKF was evaluated in the paper mill by collecting first reference fingerprints over the area where the positioning tests are carried out. 73 reference fingerprints were recorded on the operation floor and 54 fingerprints on the ground floor. The reference fingerprint grid was non-uniform with 3-5 meter spacing. Data was gathered with Fujitsu-Siemens Pocket Loox and Site Survey tool. As can be seen in Figure 63, the number of detected APs per location was 9-12 on the operation floor and 5-13 on the ground floor. Some of the APs residing on the operation floor were detected on the ground floor nearby the large hatch that is used to shift large items between the floors. Open hatch might cause temporary degradation of the positioning accuracy, since the signals from other floor would be much stronger then.

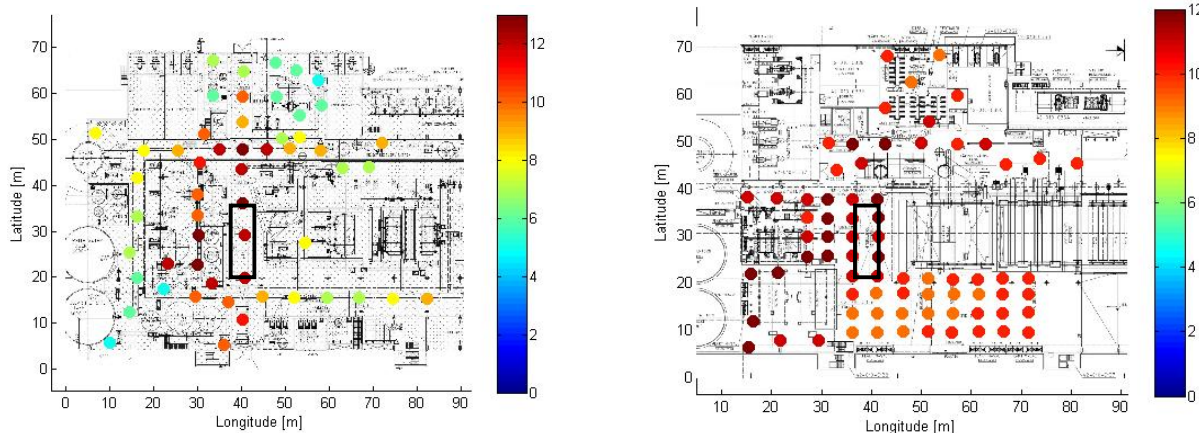


Figure 63. Reference fingerprint locations and number of detected APs in ground floor (left) and operation floor (right). Hatch connecting the two floors is marked with a black rectangle.

The test route was the learning and field operator route presented in [31]. Route was divided into operator (O) and ground floor (G) parts and it was repeated five times with Dell D820

laptop and three times with Fujitsu Siemens Pocket Loox. Accuracy statistics are presented in Table 10 .

Table 10. DCM results from the measurements carried out in Kvarnsveden paper mill.

Route:	Samples:	Mean [m]:	CEP 50% [m]:	CEP 67% [m]:	CEP 95% [m]:	Max error [m]:
D820 G1	132	5.1	4.6	5.6	9.6	16.2
D820 G2	132	5.0	5.0	5.9	9.5	11.8
D820 G3	132	4.9	4.1	5.4	10.3	14.6
D820 G4	132	5.2	5.0	5.9	10.9	13.5
Fujitsu G1	132	5.0	5.0	5.9	9.3	10.6
Fujitsu G2	132	5.2	5.0	5.9	10.0	11.8
Fujitsu G3	132	5.3	5.1	6.2	9.2	12.7
D820 O1	168	6.1	5.9	7.3	10.5	12.5
D820 O2	168	6.0	5.4	6.8	12.5	15.4
D820 O3	168	6.8	6.2	7.4	16.1	20.4
D820 O4	168	6.1	5.6	6.8	12.6	16.1
D820 O5	168	6.2	6.0	7.4	11.0	14.9
Fujitsu O1	168	4.8	4.0	5.7	9.6	17.3
Fujitsu O2	168	5.3	4.9	5.9	10.8	13.7
Fujitsu O3	168	5.0	4.5	5.4	10.7	14.9

The average accuracy using DCM is around 4-7m and maximum error is over 20m. As can be seen in Figure 64, the deployed method cannot distinguish on which side of the large corridors the user resides. After deploying Extended Kalman Filter, the route trajectory is more distinguishable. However, since the positioning errors of DCM are far from being normal distributed measurement noise, EKF fails to improve the positioning accuracy.

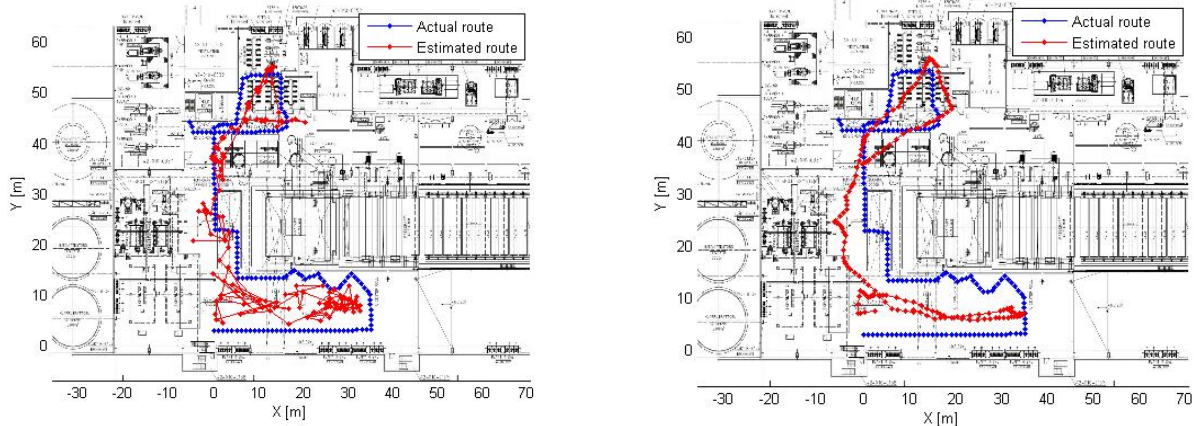


Figure 64. Operation floor route positioned with DCM (left) and DCM+EKF (right).

Similarly on the ground floor, the accuracy of DCM is sufficient to e.g. aid marker-based tracking by limiting the search of possible markers in the vicinity of the user. Showing the user location as dot on top of the floor plan accurately enough is clearly too big challenge. Actual and estimated route on the ground floor is depicted in Figure 65.

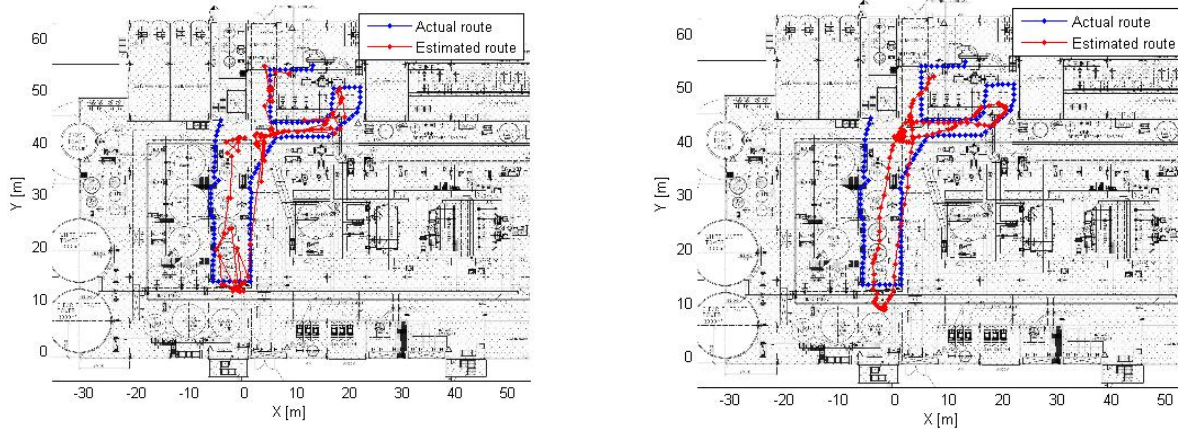


Figure 65. Ground floor route positioned with DCM (left) and DCM+EKF (right).

4.5 Sensor navigation results

The ZUPT based PDR algorithm developed in ILPO project was evaluated with MicroStrain sensor in Kvarnsveden paper mill. The test route is the same route that was used to evaluate WLAN location fingerprinting accuracy. This 168m long test route having no elevation changes was repeated five times with 1m/s walking speed. Similarly to preliminary trials carried out in Digitalo, the heading correction based on electronic compass was not yet used. As can be seen in Figure 66, the algorithm was able to predict the shape of the route quite accurately. However, errors introduced in the heading by occasional tilt errors slowly accumulate. In the best case, the location displacement at the end of the route was less than a meter and worst case around 10 meters.

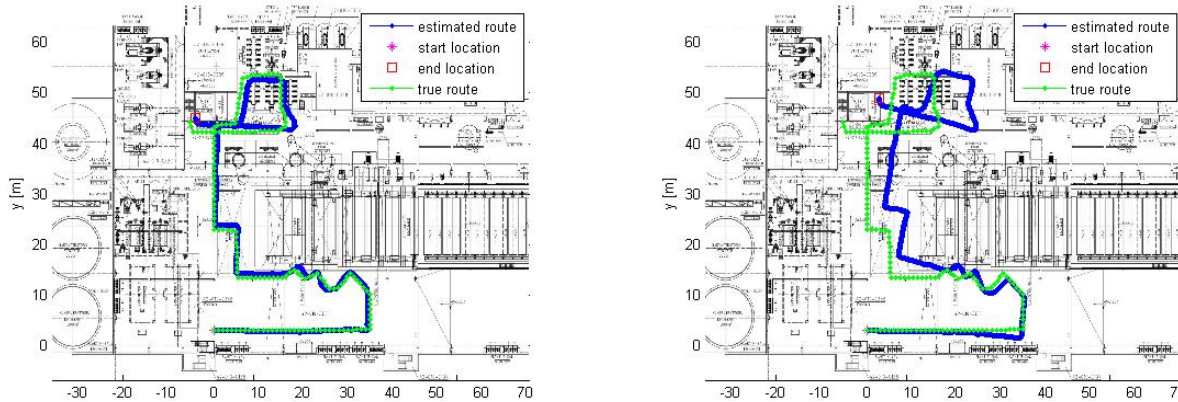


Figure 66. Route on operation floor positioned with ZUPT based PDR (initial position and heading is given to the algorithm). Best (left) and worst (right) of the five repeats.

On the ground floor, the test route was shorter (132m) but has some elevation changes: the route leads to a maintenance passageway 4 meters upstairs and then ends up back to the ground level after three shorter sections of stairs (see Figure 67). The rest of the route has no elevation changes. Due to the stairs, the walking speed was lower (0.5m/s) in order to avoid accidents in the stairs (person collecting the data had to carry a laptop without supporting rack).



Figure 67. The ground floor test route follows stairs up to the maintenance passageway (left) and leads back to the ground level after three sets of shorter stairs (right).

As can be seen in Figure 68, the algorithm was again able to predict the shape of the route quite accurately. However, errors introduced in the heading by occasional tilt errors are bigger than on the operation floor. In the best case, the location displacement at the end of the route was less around 5 meters and in worst case around 20 meters.

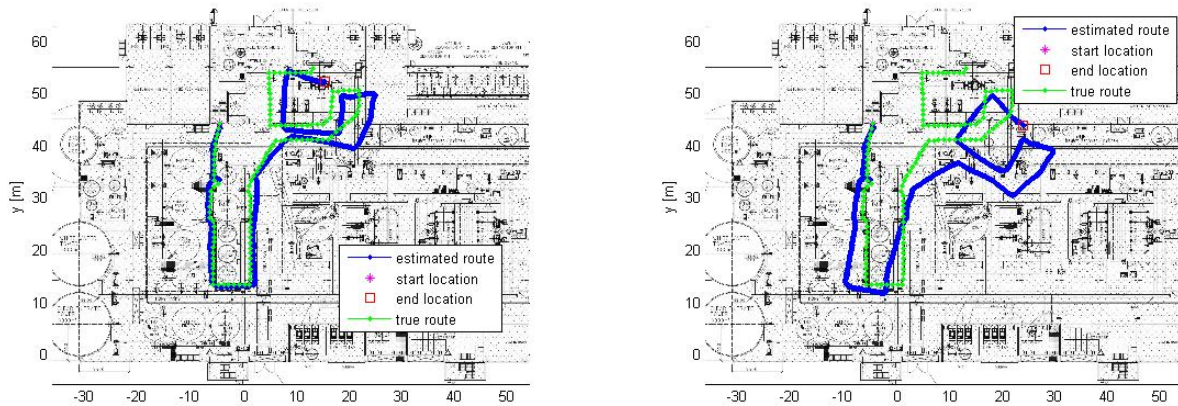


Figure 68. Route on ground floor positioned with ZUPT based PDR (initial position and heading is given to the algorithm). Best (left) and worst (right) of the five repeats.

5 Kvarnsveden pilot 2009

The second positioning pilot was carried out in Kvarnsveden paper mill on 24-26.11.2009.

5.1 Trial area

The area for the second trial equals to the area used in first trial in 2008. The same test routes were repeated to evaluate the accuracy and performance of the implemented hybrid positioning method introduced in section 2.5. Additionally data was collected from one longer route in ground floor.

5.2 Trial setup

For the trial, 13 Linksys WRT54GL WLAN access points were placed around the ground and the operation floor. All other APs existing in the area were excluded from the trial. Seven APs were set to the operation floor (see Figure 48) and the rest of the APs were distributed to the ground floor (see Figure 47). The access points were placed on the floor or on top of the electric board at 1.3 meters.

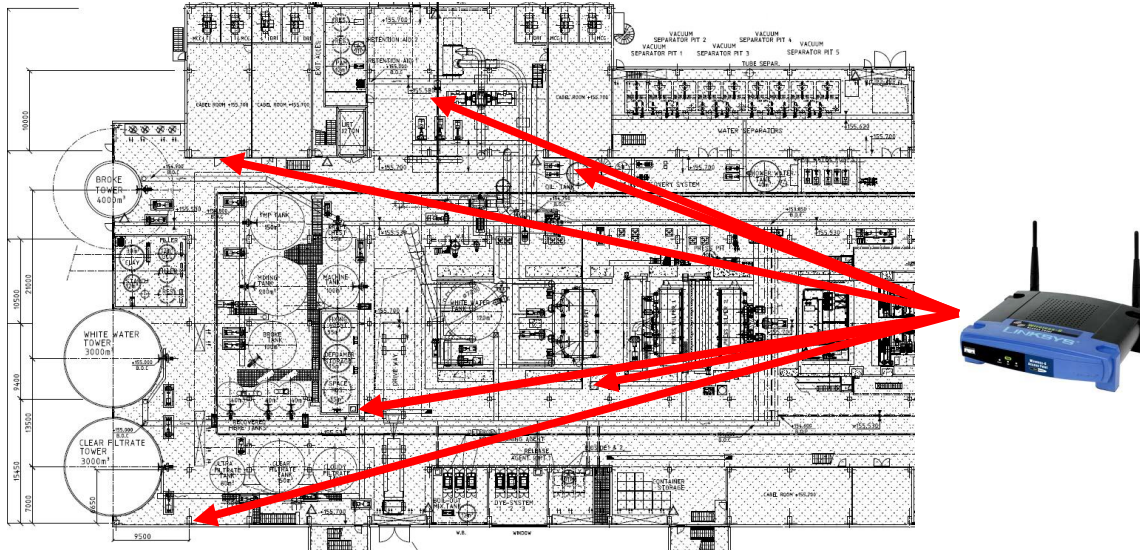


Figure 69. WLAN setup and trial area on the ground floor.

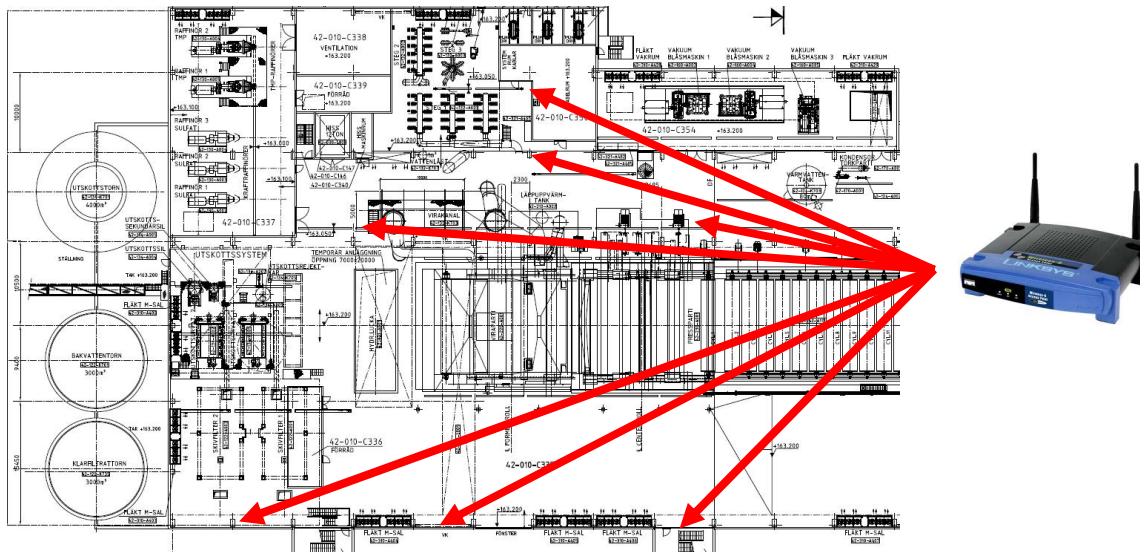


Figure 70. WLAN setup and trial area on the operation floor.

5.3 Reference image database

Reference image database was collected with *LocationDataScanner* tool. It is a script running on MATLAB allowing the user to draw routes on top of floor plan image. Reference images and corresponding WLAN signal levels are collected along the drawn routes with 1s interval which corresponds approximately 0.5m spacing between consecutive data samples. Script assumes that the user walks with constant velocity and assigns location for each sample by dividing the length of the route with the number of collected samples. Therefore, the accuracy of the assigned location information decreases if walking speed is not kept constant. The script assists the user to keep the same pace by playing a beep sound after each sample taken.

A total of 1044 reference images (and WLAN signal levels) were collected from the ground floor. The corresponding number in the operation floor was 1031. Reference image routes were walked towards both directions. Most of the data was collected from main corridors and passageways. A sequence of reference images is shown in Figure 71.



Figure 71. Reference images from operation and ground floor.

Some of the reference images were corrupted by motion blur. Despite the adjustment of camera settings, the problem still existed. Nevertheless, all the collected images were kept in the database. Some images corrupted by motion blur are depicted in Figure 72.



Figure 72. Examples of reference images corrupted by motion blur.

5.4 Hybrid positioning results

The first test route was a walk around ground floor corridors. Reference database contained images from the whole route, though the test route was not exactly the same with the reference measurement route. Marker-less vision based tracking results a total of 135 location updates. As can be seen in Figure 73, only small errors ($<1\text{m}$) are introduced because of the difference between true location and best matching reference image location. PDR estimates nicely the shape of the route during the few longer gaps between camera location updates.

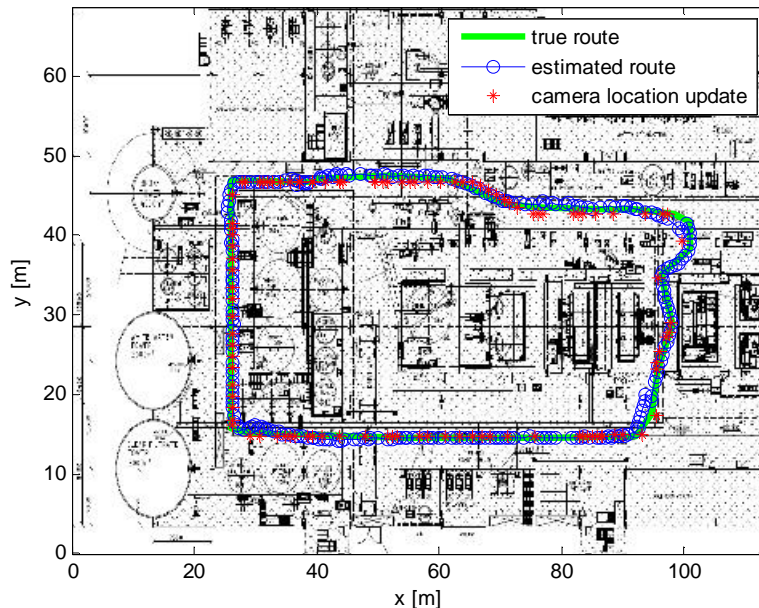


Figure 73. Test route 1, ground floor.

Test measurement route 2 equals to the ground floor part of the learning and field operator route used in the first trial carried out in 2008. Results are shown in Figure 74. The reference database does not contain images from the whole test route. Despite of this, marker-less vision based tracking yields 43 location updates which are enough to predict the route quite accurately together with PDR. PDR actually fails to estimate the travelled distance correctly at the beginning when the route leads to a maintenance passageway 4 meters upstairs and then ends up back to the ground level after three shorter sections of stairs. The step length

estimation based on step frequency clearly overestimates the step length when walking down/upstairs. Otherwise the fusion yields relatively good positioning accuracy.

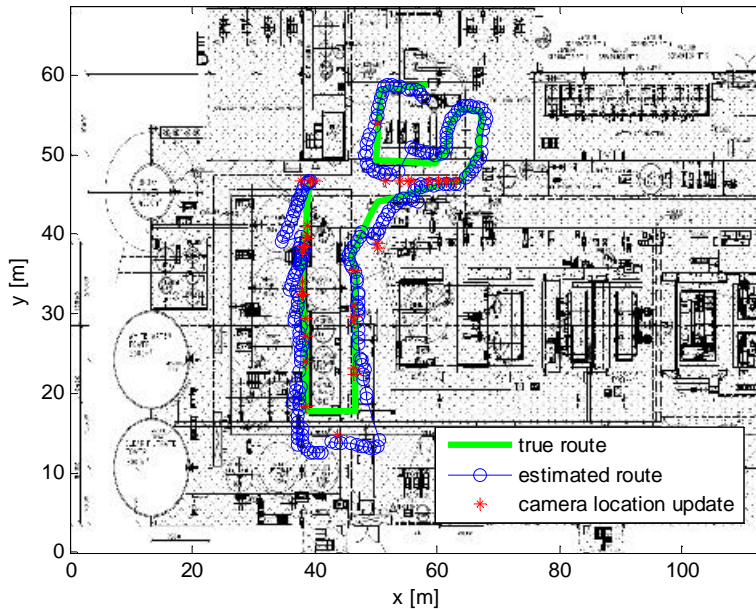


Figure 74. Test route 2, ground floor.

Last route (Figure 75) is the second half of the learning and field operator route. First camera location update is received after 7 meters of walking. After that, only few other image matches are detected when walking around the large open space next to the paper machine. During the reference database collection, the floor was filled with paper machine components waiting to be installed during the maintenance break. During the test route walks on the next day, most of the components were already cleared away. Moreover, the reference data did not contain samples from all parts of the test route. For instance, the part nearby the lower left corner of the paper machine was not covered. After fifth location update nearby the paper machine, PDR gets slightly wrong direction. Until next update is received, the estimates are few meters apart from the true trajectory. The rest of the path is estimates with <1m accuracy.

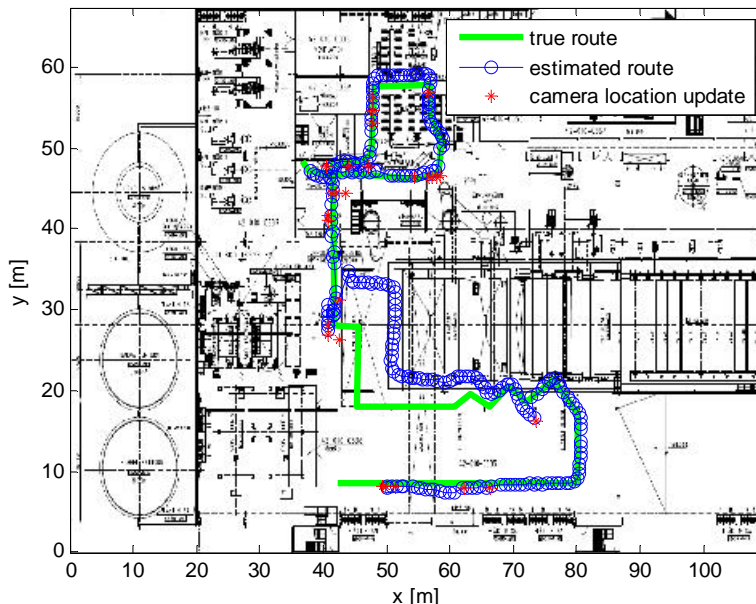


Figure 75. Test route 3, operation floor.

Conclusions

Existing positioning solutions based on different technologies were shortly reviewed and their usability and limitations for the use cases were analysed. As complementary methods, WLAN location fingerprinting, pseudolites, and inertial navigation methods were chosen for a trial. They were installed and tested in paper mill environment. The goal was to find a positioning solution that is accurate enough to be used in guidance of a field operator working in such a demanding environment as a paper mill.

Trials in Digitalo and the underground hall indicated that setting up a pseudolite positioning system is laborious. It requires a lot of planning and adjustments to ensure that the system itself doesn't cause errors to the positioning. First of all, each antenna position must be chosen carefully. After that, an optimal antenna type needs to be selected for each position. Antenna positions must also be measured as accurately as possible, and when the first setup is ready and synchronized, it needs verifications with measurements to ensure that the setup is as good as possible. The whole procedure (with the constellation of six pseudolites) takes at least three days depending on the environment and number of changes needed. When the pseudolite installation is final, it stays well synchronized unless the direct signal between the reference antenna and the pseudolites is blocked.

Results have proven that if the space is large and high enough, the pseudolite system offers pretty good tracking in open areas. The average positioning error is, in most cases with a good setup, within 3 meters. The bottleneck is the initial position estimate. If it is biased the later position estimates will usually suffer from it long before the system corrects it. Every now and then it takes quite a long time even to get the first fix and the position estimate.

WLAN location fingerprinting provides less accuracy than pseudolite systems (the mean accuracy is 4-7 m), but it can be set up with much less effort and cost. In addition, WLAN location fingerprinting works in areas where there is a no-line-of-sight between the access points and the device that is being tracked. A pseudolite system always requires a line-of-sight between at least 4 pseudolites and the receiver. This is often hard to achieve, especially in a complex indoor environment with no large open areas. WLAN location fingerprinting can be used as a complementary positioning system providing relatively coarse positioning accuracy.

The accuracy of WLAN location fingerprinting could be improved by more elaborate placing of the WLAN access points. Now the possible AP locations were limited by the availability of power outlets. Also the deployed algorithm could be replaced with more advanced probabilistic methods. However, even after adjusting the AP locations and improving the algorithm, it may well be a demanding task to achieve < 3 m mean location accuracy.

Inertial sensor based positioning algorithm developed in ILPO2 project was tested with Microstrain MEMS inertial measurement unit both in Digitalo and paper mill environment. The implemented complementary EKF for Pedestrian Dead Reckoning indicates a good tracking accuracy. However, this method alone does not provide autonomous positioning: the initial position and heading needs to be known. Moreover, the heading estimate gets slowly inaccurate due to gyroscope drift and tilt (pitch/roll) errors. The heading error could be corrected by using an electronic compass or other positioning methods to periodically fix the effects from the drift. However, the trial proves that paper mill environment is too challenging

for using electronic compass. The environment has a lot of metallic building structures, electric equipment, and power lines which cause soft and hard iron field distortion.

A hybrid positioning solution was tested in the second year trial. It comprised of marker-less vision based tracking, coarse WLAN positioning and inertial sensing (PDR). Marker-less vision based tracking worked well providing frequent location updates in all parts of the test area. The method tolerated even some radical changes in the environment (e.g. fork-lift parked in the middle of operation floor and spare parts being assembled next to the paper machine). It provided only few false image matches even though there were numerous ambiguous structures and shapes in the environment.

Coarse WLAN positioning limited effectively the search space for the marker-less tracking, and at the same time, reduced the possibility of finding false image matches from different parts of the building (e.g. similar tank found in two separate places). PDR for waist-mounted sensor provided reasonably accurate estimation of the walking trail in all the three test routes. Step length estimation based on step frequency was known to be prone to errors when walking down/upstairs. This was noticed along the ground floor route that leads to a maintenance passageway 4 meters upstairs and then ends up back to the ground level after three shorter sections of stairs. In the future, step length could be corrected in staircases by using relative altitude data based on barometric altimeter.

Fusion of marker-less vision based tracking and PDR could be improved in the future to tolerate effectively false image matches. For instance, the number of convergent features in the current camera view and best matching reference image could be used to adjust the measurement noise covariance in the Kalman filter.

The process of collecting the image database could be made easier by using PDR. User would need to give only the start and end location of the walked route and PDR would be then used to estimate the route trajectory and assign location information for the collected images and WLAN signal level data. Later, the process could be automated even more by utilizing a wireless mobile web camera to perform the data collection. Moreover, corrupted images and images with only few distinctive features could be discarded before deploying the database for positioning.

Based on the experiences gained in this project, it seems that there's no single positioning method that would enable accurate and widely available indoor positioning in challenging industrial environments. However, the requirements can be met if multiple supporting techniques are combined. The developed hybrid positioning solution is definitely a promising experiment that should be experimented and developed further.

References

- [1] El-Rabbany, A., *Introduction to GPS: The Global Positioning System*. Artech House, 2002.
- [2] Essentials of Satellite Navigation (GNSS_Compendium_English(GPS-X-02007).pdf)
<http://www.u-blox.com/technology/GPS-X-02007.pdf>
- [3] Laitinen, H., Lähteenmäki, J., Nordström, T., *Database Correlation Method for GSM Location*. Proc 53rd IEEE Vehicular Technology Conference, Rhodes, Greece, May 6-9, 2001.
- [4] Ahonen, S., Laitinen, H., *Database Correlation Method for UMTS Location*. Proc 57th IEEE Vehicular Technology Conference, Jeju, Korea, April 22-25, 2003.
- [5] Kemppi, P., Nousiainen, S., *Database Correlation Method for Multi-System Positioning*. Proc 63rd IEEE Vehicular Technology Conference, Melbourne, Australia, May 7-10, 2006.
- [6] Rosum TV-GPS, <http://www.rosum.com/>
- [7] EkaHau, <http://www.ekahau.com>
- [8] Roos, T., et al., *A probabilistic approach to WLAN user location estimation*. International Journal of Wireless Information Networks, vol. 9, no. 3, pp. 155-164, July, 2002.
- [9] Dai, L., et al., *Pseudo-Satellite Applications in Deformation Monitoring*. GPS Solutions, vol. 5, no. 3, pp. 80-87, 2002.
- [10] Kee, C., Yun, D., Jun, H., *Precise calibration method of pseudolite positions in indoor navigation systems*. Computers and Mathematics with Applications, vol. 46, pp. 1711-1724, 2003.
- [11] Petrovski, I., et al., *Pedestrian ITS in Japan: Pseudolites and GPS*. GPS World, March, 2003.
- [12] Kanli, M. O., *Limitations of Pseudolite Systems Using Off-The-Shelf GPS Receivers*. Journal of Global Positioning Systems, vol. 3, no. 1-2, pp. 154-166, 2004.
- [13] Bartone, C.G., Kiran, S., *Flight test results of an integrated wideband airport pseudolite for the local area augmentation system*. Navigation. Journal of the Institute of Navigation, vol.48, no.1, pp.35-48, 2001.
- [14] LeMaster, E.A., Rock, S.M, *A Local-Area GPS Pseudolite-Based Navigation System for Mars Rovers*. Autonomous Robots, vol.14, no.2-3, March, 2003.
- [15] El-Rabbany, A., *Mining Positioning*. Proc. Smart Systems for Mineral Resources Workshop, Toronto, Ontario, February 14, 2001.
- [16] Kee, C., Jun, H., Yun, D., *Indoor Navigation System using Asynchronous Pseudolites*. Journal of Navigation, vol. 56, pp. 443-455, 2003.
- [17] *GSG-L1 GPS Signal Generator User's Manual*. Naviva, May 2007.
- [18] *EGNOS Pseudolite System MCS Manual*. Space Systems Finland, November, 2006.
- [19] Laitinen, H., Ström, M., *Single-frequency Carrier Navigation in a Synchronised Pseudolite Network*, ENC-GNSS 2009, May, 2009.
- [20] Petrovski, I., et al., *Precise Navigation Indoor*. SICE Annual Conference in Sapporo, August 4-6, 2004.
- [21] Lee, H. K., et al., *GPS/Pseudolite/INS integration: concept and first tests*. GPS Solutions, vol. 6, pp. 33-46, 2002.

- [22] Foxlin, E., *Pedestrian tracking with shoe-mounted inertial sensors*. IEEE Computer Graphics and Applications, vol. 25, no. 6, pp. 38–46, 2005.
- [23] Weimann, F., Abwerzger, G., Hofmann-Wellenhof, B., *Let's Go Downtown! Let's Go Indoors! Pedestrian Navigation in Obstructed Environments*. GPS World, November, 2007.
- [24] Vildjounaite, E., et al., *Location Estimation Indoors by Means of Small Computing Power Devices, Accelerometers, Magnetic Sensors, and Map Knowledge*. Proc. Proceedings of the First International Conference on Pervasive Computing 2002, pp. 211-224, 2002.
- [25] Youssef, M., Agrawala, A., *Handling samples correlation in the Horus system*. INFOCOM 2004, Twenty-third Annual Joint Conference of the IEEE Computer and Communications, vol.2, 7-11, pp. 1023- 1031, March, 2004.
- [26] Youssef, M., *HORUS: WLAN Based Indoor Location Determination System*. PhD thesis, University of Maryland at College Park, May, 2004.
- [27] Kourogi, M., Kurata, T., *Personal positioning based on Walking Locomotion Analysis with Self-Contained Sensors and Wearable Camera*. Proc. ISMAR, 2003.
- [28] Evennou, F., Marx, F., Novakov, E., *Map-aided indoor mobile positioning system using particle filter*. Proc. IEEE Wireless Communications and Networking Conference (WCNC '05), vol. 4, pp. 2490–2494, New Orleans, La, USA, March, 2005.
- [29] Widyan, Klepal, M., Beauregard, S., *A backtracking particle filter for fusing building plans with PDR displacement estimates*. Proceedings of the 5th workshop on positioning, navigation and communication 2008 (WPNC'08), pp. 207-212, 2008.
- [30] Woodman, O., Harle, R., *Pedestrian Localisation for Indoor Environments*. Proceedings of the UbiComb'08, September, 2008.
- [31] NOSE Technology Report, VTT

ANNEX 1: MicroStrain 3DM-GX2 specifications

MicroStrains 3DM-GX2, includes three sensors: a triad gyroscope, a triad accelerometer, and a triad magnetometer aligned along common axes. A fourth sensor, a thermometer, is used for calibrating the outputs with respect to temperature, and the operating area is -40°C to +70°C. The accelerometer has a dynamic range of ± 5 g, the gyroscope a range of ± 600 deg/s, and the magnetometer a range of ± 1.2 Gauss. The sensor system can provide 6-DOF (Degrees of Freedom) motion tracking. This refers to movements in x-, y-, and z-axis directions as well as rotational movements around these axes (see Figure 76).

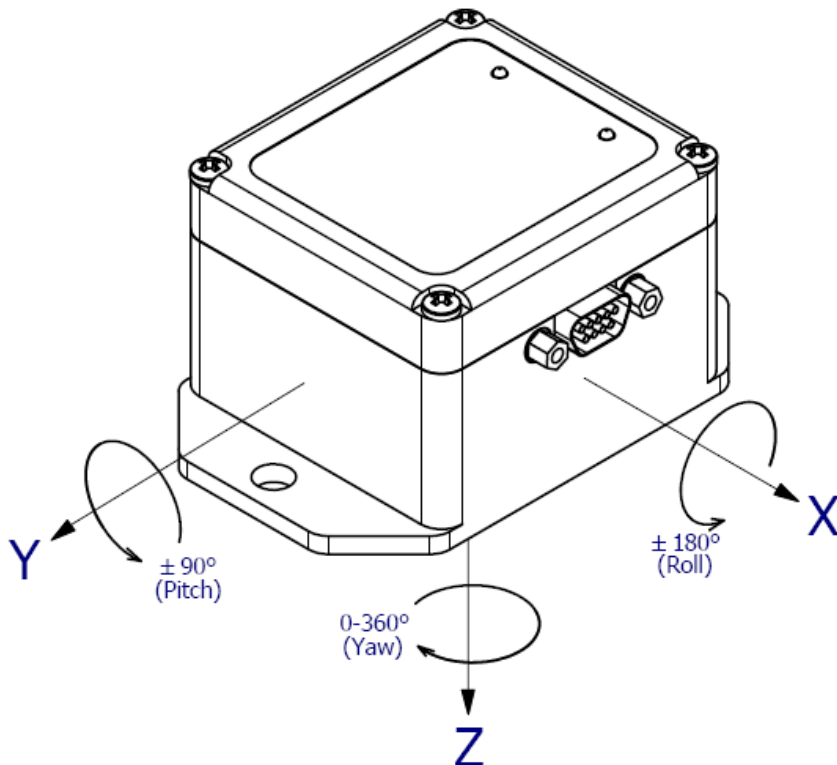


Figure 76. MicroStrain 3DM-GX2 axes, ©MicroStrain.

Table 11. Accuracy of 3DM-GX2 sensors found from specifications and calibration tests.

	Accelerometers	Gyroscopes	Magnetometers
Range (promised in specs)	± 5 g / ± 10 g / ± 2 g ??	$\pm 300^\circ/\text{s}$ OR $\pm 1200^\circ/\text{s}$ OR $\pm 600^\circ/\text{s}$??	± 1.2 Gauss
Bias stability (promised in specs)	± 0.01 g / ± 0.005 g / ??	720°/h for $\pm 300^\circ/\text{s}$	0.01 Gauss
Bias stability (through tests)	x: ± 0.00003 g y: ± 0.00008 g z: ± 0.00003 g	x: 24°/h y: 22°/h z: 138°/h	
ARW (through tests)	x: 0.00079 m/s $\sqrt{\text{s}}$ y: 0.00097 m/s $\sqrt{\text{s}}$ z: 0.00093 m/s $\sqrt{\text{s}}$	x: 0.028 °/ $\sqrt{\text{s}}$ = 1.7 h y: 0.029 °/ $\sqrt{\text{s}}$ = 1.7 h z: 0.044 °/ $\sqrt{\text{s}}$ = 2.6 h	
Nonlinearity (promised in specs)	0.2%	0.2%	0.4%